Regenerative Engineering and Translational Medicine (2020) 6:451–483
https://doi.org/10.1007/s40883-019-00132-3

ORIGINAL RESEARCH

Bioinspired Scaffold Designs for Regenerating Musculoskeletal Tissue Interfaces

Mohammed A. Barajaa[1,2] · Lakshmi S. Nair[1,2,3,4,5,6,7] · Cato T. Laurencin[1,2,3,4,5,6,7,8]

Received: 10 June 2019 / Revised: 14 August 2019 / Accepted: 13 September 2019 / Published online: 17 December 2019

Abstract

The musculoskeletal system works at a very advanced level of synchrony, where all the physiological movements of the body are systematically performed through well-organized actions of bone in conjunction with all the other musculoskeletal soft tissues, such as ligaments, tendons, muscles, and cartilage through tissue-tissue interfaces. Interfaces are structurally and compositionally complex, consisting of gradients of extracellular matrix components and cell phenotypes as well as biochemical compositions and are important in mediating load transfer between the distinct orthopedic tissues during body movement. When an injury occurs at interface, it must be re-established to restore its function and stability. Due to the structural and compositional complexity found in interfaces, it is anticipated that they presuppose a concomitant increase in the complexity of the associated regenerative engineering approaches and scaffold designs to achieve successful interface regeneration and seamless integration of the engineered orthopedic tissues. Herein, we discuss the various bioinspired scaffold designs utilized to regenerate orthopedic tissue interfaces. First, we start with discussing the structure-function relationship at the interface. We then discuss the current understanding of the mechanism underlying interface regeneration, followed by discussing the current treatment available in the clinic to treat interface injuries. Lastly, we comprehensively discuss the state-of-the-art scaffold designs utilized to regenerate orthopedic tissue interfaces.

Lay Summary

Orthopedic tissues are connected to one another through interfaces that play an important role in transitioning mechanical loads between the disparate tissues. After an injury, interfaces must be re-established in order to restore joint function and stability. Understanding the mechanism governing the development of interfaces may lead to successful interface re-establishment and scaffold designs. This article discusses the current knowledge of the structure-function relationship at the interface, the mechanism underlying interface regeneration, and the current treatment available in the clinic to treat interface injuries, as well as bioinspired scaffold designs and engineering strategies to regenerate the complex orthopedic tissue interfaces.

Keywords Regenerative engineering · Tissue-tissue interfaces · Multi-tissue units · Gradient scaffolds · Stratified scaffolds · Zonal transition · Structural heterogeneity · Cellular heterogeneity · Compositional heterogeneity

✉ Cato T. Laurencin
laurencin@uchc.edu

[1] Connecticut Convergence Institute for Translation in Regenerative Engineering, University of Connecticut Health Center, Farmington, CT 06030, USA

[2] Department of Biomedical Engineering, University of Connecticut, Storrs, CT 06269, USA

[3] Raymond & Beverly Sackler Center for Biomedical, Biological, Physical & Engineering Sciences, University of Connecticut Health Center, Farmington, CT 06030, USA

[4] Department of Orthopedic Surgery, University of Connecticut Health Center, Farmington, CT 06030, USA

[5] Department of Materials Science & Engineering, University of Connecticut, Storrs, CT 06269, USA

[6] Institute of Materials Science, University of Connecticut, Storrs, CT, USA

[7] Department of Chemical & Bimolecular Engineering, University of Connecticut, Storrs, CT 06269, USA

[8] Department of Craniofacial Sciences, School of Dental Medicine, University of Connecticut Health Center, Farmington, CT 06030, USA

Introduction

Human organs are comprised of diverse tissue types that interface with each other and operate in synchrony to enable complex functions [1]. Musculoskeletal system, for instance, works at a very advanced level of synchrony, where all the physiological movements of the body are systematically performed through very well-organized actions of bone in conjunction with all the other musculoskeletal soft tissues, such as ligaments, tendons, muscles, and cartilage [1]. These tissues are well connected to each other through tissue-tissue interfaces, which act as bridging units between the distinct orthopedic tissue types [1]. Interfaces demonstrate well defined spatial change in cellular phenotype and extracellular matrix composition, as well as mechanical properties (Fig. 1) [2]. This spatial change is crucial in mediating load transfer during body movement, as well as sustaining the heterotypic cellular communications required for interface function and homeostasis [2]. When an injury occurs at the interface, it must be re-established to restore its function and stability.

Clinically, interface injuries are treated using biological grafts such as autografts, known as the transplantation of tissue within an individual from a donor site to the injury site, or allografts, known as the transplantation of tissue or a whole organ from another individual or a cadaver [3]. Although biological grafts are considered the gold standard in today's medicine, they possess a number of drawbacks which make them risky to use or undesirable for long-term use [3]. For instance, autografts cause pain and related complications to patients whereas allografts pose the risk of disease transmission and

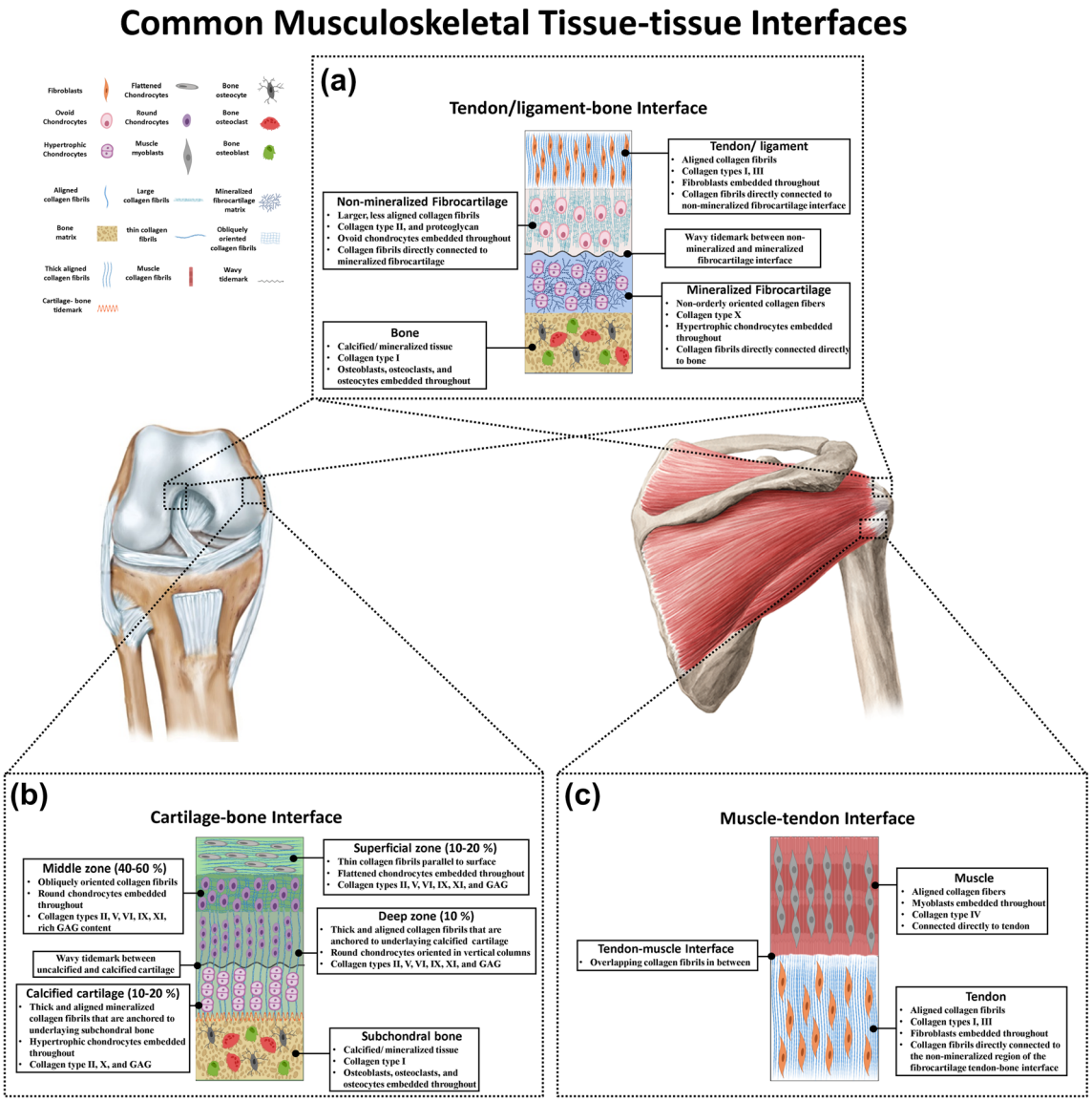

Fig. 1 Ultrastructure of the common musculoskeletal tissue-tissue interfaces. (A) Tendon/ligament-bone, (B) cartilage-bone, and (C) muscle–tendon interfaces and their compositions

immune-rejection [4]. Moreover, due to the structural and compositional complexity found at the interfaces, the conventional clinical surgical approaches cannot re-establish their function after surgery, leading to high rates of re-rupture due to poor integration between soft tissue and bone [5]. In addition to biological grafts, there are a limited number of artificial grafts that have been FDA-approved and undergone human clinical trials [6–10], but are inferior to currently used biological grafts due to the inconsistent outcomes between patients and inability to recapitulate the complexity found at the native interface, which limits their clinical use [11–14].

Alternatively, regenerative engineering represents a new paradigm for regenerating complex tissues and seamlessly integrating them into organ systems through the utilization of the most advanced technologies currently available in distinct fields such as advanced materials science, stem cell science, developmental biology, physics, and translational medicine [3]. It is anticipated that increasing the levels of complexity in tissues or organs targeted for repair presupposes a concomitant increase in the complexity of the associated regenerative engineering approaches and scaffold designs [15]. Hence, one of the main advantages presented in this field is that it focuses on mimicking the physical, chemical, mechanical, and complex topographical properties found at the native tissues into the scaffold design for integrative and natural regeneration [16].

To achieve a successful scaffold design, it is of paramount importance to understand the structure-function relationship of tissues targeted for repair and the mechanisms governing their development and regeneration, such as those of the tissue-tissue interfaces [17]. Ideally, an interfacial scaffold should be multi-phased to recapture the multi-tissue organization observed at the tissue-tissue interface. The scaffold should also exhibit phase-specific structural, compositional, and material properties to stimulate cellular response such as proliferation and differentiation [18]. The scaffold should also exhibit a gradual increase in mechanical properties across the scaffold phases, similar to those found at the native tissue in order to eliminate the formation of stress concertation [18]. In addition, the scaffold should introduce a spatial control over mineral distribution across the distinct phases, which can control the mechanical heterogeneity at the interface [18]. The length of the interface targeted for repair should also be considered into the scaffold design, which can vary in length (sub-millimeter-micrometers scale) depending on gender, age, body mass index (BMI), species, and interface type [19, 20]. To better sustain the load transfer across the scaffold, the scaffold should be pre-integrated. The scaffold should also exhibit phase-specific surface properties to support the phase-specific relevant cell performance [18]. Considering all of these parameters may enable the creation of optimal scaffold designs with intrinsic properties, which in turn may accelerate their translation into the clinic. In this review paper, we discuss the current knowledge of the structure-function relationship at the interface and the mechanism underlying interface regeneration. We also discuss the available clinical approaches to re-establish injured interfaces, followed by a comprehensive discussion and evaluation of the current state-of-the-art bioinspired scaffold designs and engineering approaches to regenerate the complex orthopedic tissue interfaces (e.g., ligament-bone interface, tendon-bone interface, and muscle-tendon interface, as well as cartilage-bone interface).

Ligament-Bone Interface

Ligament-Interface-Bone Structure and Function

Ligament is a soft tissue that connects bone to bone through a characteristic fibrocartilage interface, with a controlled spatial change in cell phenotype, extracellular matrix composition, and mechanical properties. Three distinct regions are found along the bone-ligament junction: ligament, fibrocartilage interface, and bone. The fibrocartilage interface is further divided into mineralized and non-mineralized fibrocartilage zones [17], where ligament is directly connected to the non-mineralized region of fibrocartilage and the mineralized region is directly connected to bone [5]. Within the ligament tissue, ligament fibroblasts are found entrapped in collagen type I and III matrix [17]. At the non-mineralized region of the fibrocartilage interface, ovoid chondrocytes are found entrapped in collagen type II proteoglycan-rich matrix. At the mineralized region, heterotrophic chondrocytes are found entrapped in collagen type X calcified matrix. At the bony region, referred to as the "subchondral bone," osteoblasts, osteoclasts, and osteocytes are found embedded into a mineralized collagen type I matrix. This cellular heterogeneity found along the bone-ligament insertion area plays a key role in permitting the gradual transition of mechanical loads between soft tissues and bone, which decreases the concentration of stress formation during body movement [21, 22].

Current Understanding of the Mechanism Underlying Tendon/Ligament-Bone Interface Development and/or Regeneration

The mechanism governing tendons/ligaments-bone interface development and regeneration is yet to be well understood. In the clinic, it has been long observed that re-suturing tendon into its original insertion site results in cellular organization resembling that of the native interface in vivo [18]. This has been further emphasized by Fujioka et al. when cellular organization at the native insertion site has been observed over time after an Achilles tendon is re-sutured to its original attachment site [23]. These intriguing observations led to the hypothesis that the interactions between the resident cell

populations (e.g., tendon/ligament fibroblasts) and (e.g., bone osteoblasts) play a crucial role in initiating the repair response which leads to the regeneration of the fibrocartilage interface between bone and soft tissue [24]. It was further hypothesized that fibroblasts-to-osteoblasts interaction interpose interface regeneration through two mechanisms: (1) osteoblasts, fibroblasts, or both undergo trans-differentiation or phenotypic changes, and (2) progenitor stem cells or mesenchymal stem cells (MSCs) recruit to the graft-bone interface, where they differentiate into fibro-chondrocytes and form the fibrocartilage interface [24].

To examine the aforementioned hypothesis and observations, one study made an attempt to mimic the in vivo interactions between fibroblasts and osteoblasts during anterior cruciate ligament (ACL) reconstruction by creating a co-culture system in vitro. In this system, a hydrogel divider was added in the middle of the culture well that separated the well into two equal chambers. Fibroblasts were seeded in one chamber, and osteoblasts were seeded in the other chamber [25]. When both cells reached confluence, the divider hydrogel was removed allowing the cells to migrate and interact at the interface region, which resulted in the formation of fibrocartilage-like region. These findings suggest that heterotopic cellular communications may play a key role in inducing the regenerative response that leads to the regeneration of the fibrocartilage interface between soft tissue and bone [25].

Although the regeneration mechanism of the different tendons and ligaments is similar, their rate of regeneration vary. Several reports have shown that different tendons/ligaments regenerate at different rates [26–32] and that combined tendon/ligament injuries regenerate at a slower rate compared with isolated injures and produce tissue of lower quality [26, 27, 33–37]. It has been also shown that there can be some variability in the rate of regeneration within combined and isolated tendons/ligaments (e.g., ACL and medial collateral ligament (MCL); Achilles tendon and rotator cuff) [38–48]. The reason of the variability in the rate of regeneration between these tissues is not clear but was suggested to be attributed to the local microenvironment causing alteration in their rate of regeneration, the different load regiment undertaken by tendons/ligaments based on their anatomical locations, or to what interventions they were employed to after the injury [49, 50].

Current Clinical Treatment for Ligament-Bone Interface Injuries

ACL is the most common ligament prone to injury among all the other ligaments throughout the body and requires an immediate medical intervention upon injury due to its poor self-healing potential. Several clinical approaches have been adapted for ACL reconstruction. Generally, ACL reconstruction is done by completely removing the ruptured ACL, followed by replacement with an autograft from the patient own body (e.g., the hamstring tendon (HS) or bone-patellar tendon-bone (BPTP)), or an allograft from another individual or a cadaver [51]. Although these approaches have been successful in most cases, they possess a number of drawbacks [3]. For instance, autografts cause donor-site morbidities such as a decrease in knee flexion strength and tibial rotation, as well as the possibility of sciatic or saphenous nerve damage during harvesting the autograft, whereas allografts pose the risk of disease transmission and/or immune rejection [4]. In addition, current clinical approaches for ACL reconstruction mostly focus on the restoration of the ligament but not the interface. Interface is an important unit that bridges between ligament and bone, and its establishment is important to facilitate proper graft integration to the bone. Unfortunately, current clinical approaches cannot re-establish proper interface function after surgery, leading to high rates of re-injury due to poor integration between soft tissue and bone [5].

Bioinspired Scaffold Designs for Ligament-Bone Interface Regeneration

Several simple and complex scaffold designs have been developed and employed aiming to functionally regenerate the complex ligament-bone interface. These include bi-phasic and multiple-phasic scaffold designs in the form of stratified or gradient (summarized in Table 1). Our research group developed a bi-phasic ACL graft system composed of braided poly (lactic-co-glycolic acid) (PLGA) microfibers at the center of the graft for ligament regeneration, with two denser fiber regions at either end of the graft to facilitate bone ingrowth and osteointegration [52]. In vitro evaluations demonstrated the high biocompatibility of the graft. When testing the mechanical properties of the graft under tensile, it exhibited similar properties to that at the native tissue [53]. In vivo evaluations showed a great healing potential, when collagenous tissue infiltration after 12 weeks has been observed [54]. In a similar approach, Altman et al. developed a highly porous bi-phasic silk graft system for ACL reconstruction. The graft system consisted of multiple regions with different orientations, where the middle region consisted of aligned yarns for ligament regeneration that are densely connected to knitted yarns at either end for bony integration. The graft system was evaluated in a goat ACL reconstruction model, resulting in the formation of collagenous like structure with cell alignment after 12 months of implantation at the ligament region of the graft, with good osteointegration [55].

Despite the advances represented by the bi-phasic scaffold design, a true ligament-bone interface regeneration was not evident due to the fact that incorporating an interface-specific region to the scaffold design was not put into accounts, which is crucial to enable the regeneration of the fibrocartilage interface between ligament and bone. The

Table 1 Bioinspired scaffold designs utilized for regenerating ligament-bone interface

Scaffold type	Scaffold design	Material/s used	Fabrication method	Cell type/s	Growth factor/s	Animal model	Results	Ref
Bi-phasic (gradient)	Microfibers at the center of the graft for ACL regeneration, with two denser fiber regions at either end of the graft to facilitate bone ingrowth and osteointegration	PLGA	Three-dimensional braiding technology	Primary rabbit ACL cells	N/A	Rabbit ACL reconstruction model	In vitro evaluations demonstrated the high biocompatibility of the graft, ligament tissue ingrowth as well as initial mechanical properties approximate to those of the native ligament. In vivo evaluations showed a great healing potential, when collagenous tissue infiltration after 12 weeks has been observed	[52–54]
Bi-phasic (stratified)	Yarns at the middle of the graft, which densely connects two knitted regions at either end for osteointegration	Silk	Custom-designed extraction method on a rack	N/A	N/A	Goat ACL reconstruction model	The graft resulted in the formation of collagenous like structure with cell alignment after 12 months	[55]
Bi-phasic (stratified)	Braided bioabsorbable fibers at the middle wrapped with a natural-based membrane for ACL regeneration, with hydrogel carrier for interface regeneration and osteointegration at either end	PLLA-collagen and gelatin	Three-dimensional braiding technology	N/A	bFGF	Rabbit ACL reconstruction model	In vivo evaluations revealed that the scaffold design supported the formation of ligament as well as bone at the tunnel, with the formation of an interface-like tissue in between	[56]
Bi-phasic (gradient)	Gradient electrospun scaffold consisting of two phases, a mineralized phase for bone regeneration, and a non-mineralized phase for ligament regeneration	PCL/HA	Electrospinning	BMSCs	N/A	N/A	Gradients in mineral content could guide the formation of phenotypic gradients and could promote the regeneration of ligament-bone interface. BMSCs seeded on the mineralized region had higher expression levels of BMP-2, ALP, osteopontin, and bone sialoprotein, when compared to the interface and the ligamentous regions, confirming their osteoblastic phenotypic maturation	[57]
Scaffold type	Scaffold design	Material/s used	Fabrication method	Cell type/s	Growth factor/s	Animal model	Results	Ref
Bi-phasic (gradient)	Gradient electrospun scaffold consisting of a region of aligned nanofibers for ligament regeneration, contiguous with a region of unaligned nanofibers for bone regeneration; with continues gradation in fiber orientation, diameter, chemistry, and mechanical properties throughout.	PCL/PLGA	Electrospinning	BMSCs	N/A	N/A	The gradation in fiber orientation, diameter, chemistry and mechanical properties guided the differentiation of BMSCs seeded along the scaffold into fibroblasts and osteoblasts in the respective regions	[58]

Table 1 (continued)

Scaffold type	Scaffold design	Material/s used	Fabrication method	Cell type/s	Growth factor/s	Animal model	Results	Ref
Tri-phasic (stratified)	Pre-integrated continues phases. Phase A, B and C for ligament, interface, and bone regeneration, respectively	Phase A: polyglactin, Phase B: PLGA, and Phase C: PLGA and 45S5 BG	Phase A: segments sintering of the polymeric mesh, Phase B and C: heat sintering of the polymeric microspheres	Phase A: primary ligament fibroblast, Phase B: primary chondrocytes, and Phase C: primary osteoblasts	N/A	Subcutaneous in athymic rat model.	Tri-culturing the three different cell types resulted in an extensive collagen rich-matrix production at the three different phases comparing to the co-culture system (phases A and C seeded only). In addition, formation of fibrocartilage-like tissue at the interface region containing collagen types I and II as well as glycosaminoglycans was observed	[59–61]
Tri-phasic (gradient)	Synthetic-based scaffold consisting of different pore size gradients along the three regions, where the largest pore size is at the bony region, with a gradual decrease in pore size as transitioned to the ligamentous region	PCL	Centrifugation method	Osteoblasts, chondrocytes, and fibroblasts seeded on the three scaffold regions, respectively	N/A	Rabbit skull bone defect model.	In vitro evaluations revealed that different pore sizes could strongly affect cell behaviors such as proliferation and cell fate. Osteoblasts and chondrocytes showed increased in cell number at regions with pore sizes 380–405 μm, while fibroblasts were more localized at areas with pore sizes of 186–200 μm. In vivo evaluations revealed that bone formation was evident at areas with larger pore	[62]
Scaffold type	Scaffold design	Material/s used	Fabrication method	Cell type/s	Growth factor/s	Animal model	Results	Ref
Tri-phasic (stratified)	A scaffold knitted and rolled to resemble the structure of the native ligament-bone junction, with specified regions for ligament, interface and bone regeneration	Silk	Knitting technique	BMSCs, chondrocytes and osteoblasts were respectively seeded on the three scaffold phases, respectively.	N/A	Rabbit ACL reconstruction model	In vitro evaluations showed that the tri-lineage cells loaded on the tri-phasic silk scaffold had high proliferative capacity as well as enhanced differentiation ability when seeded into their respective regions. In vivo evaluations revealed that silk-based ligamentous graft exhibited enhanced osteointergation, as well as formation of the three tissues with conspicuously corresponding matrix deposition	[63]
Tri-phasic (stratified)	Pre-seeded natural-based gel added around and bridging two growth factors soaked and prefabricated	β-TCP/fibrin gel	Custom fabrication method	Human ACL fibroblasts	BMP-2, BMP-4, BMP-7	N/A	Of the five chondrogenic growth factors (BMP-2, BMP-4, and BMP-7 and TGF-β1 and TGF-β3) tested, local release of	[64]

Table 1 (continued)

Scaffold type	Scaffold design	Material/s used	Fabrication method	Cell type/s	Growth factor/s	Animal model	Results	Ref
	brushite cement anchors that are 12 mm apart.				TGF-β1 TGF-β3		BMP-4 at the enthesis of engineered ligament improved the interface failure load by up to 38% compared with the other growth factors. BMP-4 treatment increased the expression of the enthesis-related genes Sox9, aggrecan, and tenascin C and the inhibitor of mineralization osteopontin	
Tri-phasic (stratified)	Electrospun nanofiber scaffold with gradual change from randomly aligned nanofibers for bone regeneration, to slightly aligned for interface regeneration, into highly aligned for ligament regeneration; with gradual variation in the content of osteoinductive factors and minerals	PLGA-HA/PLLA	Electrospinning	MC3T3	BMP-2	Rabbit ACL reconstruction model	The gradient nanofibrous scaffolds were found to regulate cellular morphology and zonal bone-specific differentiation in vitro. The incorporation of microfibers significantly improved the mechanical property of the gradient nanofibrous scaffolds, which was similar to native ACL-bone fixation after implantation in vivo. Histological observations revealed that the gradient scaffold facilitated the formation of fibrocartilage transitional zone as well as bone attachments that are similar to native ligament-to-bone interface.	[65]
Scaffold type	Scaffold design	Material/s used	Fabrication method	Cell type/s	Growth factor/s	Animal model	Results	Ref
Tri-phasic (gradient)	3-D printed /electrospun synthetic-based scaffold with three different regions. Highly porous 3-D printed region for bone regeneration, highly porous 3-D printed region incorporated with aligned electrospun nanofibers for interface regeneration, and aligned electrospun nanofibers for ligament regeneration, respectively.	PCL	3-D printing, and electrospinning	hMSCs	N/A	N/A	Cells seeded along the scaffold were metabolically active. ALP activity was the highest in the bone region. GAG deposition was the highest at the interface region.	[66]
Tri-phasic (gradient)	Natural-based knitted and growth factor incorporated scaffold rolled to resemble the structure of the native ligament-bone junction,	Collagen-silk (CSF)	Knitting technique	Ligament-derived stem/progenitor cells (LSPCs)	Stromal cell--derived	Rabbit ACL reconstruction model	CSF scaffold displayed a controlled release pattern for the encapsulated protein for up to 7 days with an increased stiffness	[67]

Table 1 (continued)

Scaffold type	Scaffold design	Material/s used	Fabrication method	Cell type/s	Growth factor/s	Animal model	Results	Ref
	with specified regions for ligament, interface and bone regeneration				factor 1 (SDF-1)		in the mechanical property. Injection of LSPCs, 7 days after implantation increased the expression of collagen type 1 and CXCR4 after 1 month. At 3 and 6 months post-implantation, the CSF scaffold combined with LSPCs (CSFL group) enhanced the regeneration of ACL tissue, and promoted bone tunnel healing.	
Scaffold type	Scaffold design	Material/s used	Fabrication method	Cell type/s	Growth factor/s	Animal model	Results	Ref
Five-phasic (gradient)	Aligned electrospun nanofibers at the middle of the construct for ligament regeneration, mineralized aligned electrospun nanofibers at either end of the construct for bone regeneration, and a bi-phasic nanofiber collar consisting of a region of mineralized and non-mineralized regions for interface regeneration	PCL-PLGA85:15/HA-ceramic	Electrospinning	MSCs	N/A	Rat ACL reconstruction model	In vitro evaluations revealed that increased cell density throughout led to an enhanced response due to greater cell-cell and cell-material interactions. In vivo evaluation of the synthetic ACL scaffold showed that the nanofiber-based graft was well-tolerated, with minimal inflammatory response, and reduced the duration of the reconstruction procedure, accelerating bone formation at the mineralized region, production of a GAG-containing tissue at the interface region, and most importantly, the formation of a structurally integrated multi--tissue, bone-ligament-bone junction	[68]

N/A, not available

fibrocartilage interface is optimized to withstand the tensile and compressive loading distributions along the ligament-bone junction, and thus, it plays a critical role in transitioning mechanical loads between bone and soft tissues, which as a result protects the soft tissues from the contact deformation and damage at high strains [69–73]. Inspired by the native ligament-bone interface, Spalazzi et al. reported a tri-phasic stratified scaffold design that was hypothesized to re-establish the formation of the ligament-bone interface considering the mechanical and morphological transition in the native interface extracellular matrix (ECM), as well as the relevant cell heterogeneity found along the complex tissues [59]. The tri-phasic scaffold consists of three different pre-integrated continues phases, each engineered for the regeneration of a specific tissue type, ligament, fibrocartilage interface, and bone. Phase A is made from polyglactin (10:90) knitted mesh to support ligament fibroblasts culture for the regeneration of ligament, phase B is made from PLGA (85:15) microspheres to support fibro-chondrocytes culture for the regeneration of fibrocartilage interface, and phase C is made from PLGA (85:15) sintered microspheres and 45S5 bioactive glass (BG) to support osteoblasts culture for bone regeneration [60]. The three different phases were assembled and heat sintered for pre-integration [60]. Pre-integrating the scaffold to form a multi-phased graft system was essential in order to allow for cellular interaction and to support the multiple tissue regions observed across the native ligament-bone junction [61].

For ligament and bone formation, fibroblasts and osteoblasts were seeded in phases A and C, respectively. Cellular interactions in the co-cultured tri-phasic scaffold have been evaluated both in vitro and in vivo. In vitro cell interaction evaluations revealed that the controlled cell distribution resulted in the formation of cell type–specific matrix on each phase of the scaffold. In addition, phase C was found to be mineralized, and an extensive deposition of collagen type I was found in both phases A and B [60]. In vivo evaluations in a nude rat subcutaneous model revealed that the co-cultured tri-phasic scaffold supported multilineage cellular interactions as well as tissue infiltration with abundant specific-matrix production in phases A and C. Moreover, cell migration from both phases to phase B was observed along with vascularity and matrix production [61].

The tri-phasic scaffold system was further in vivo evaluated in the same animal model for the potential to form fibrocartilage-like tissue at the interface region. This was done by tri-culturing the three different cell types, fibroblasts, chondrocytes, and osteoblasts, along the three different phases and comparing the findings to the co-culturing system. Specifically, fibroblasts were seeded on phase A, chondrocytes were seeded on phase B, and osteoblasts were seeded on phase C, respectively. Tri-culturing the three different cell types resulted in an extensive collagen rich–matrix production at the three different phases comparing to the co-culture system. In addition, formation of fibrocartilage-like tissue at the interface region containing collagen types I and II as well as glycosaminoglycans was observed. Mechanical properties of the tri-phasic scaffold were evaluated in vivo both after the co-culture and tri-culture experiments resulting in improved mechanical gradient with the highest elastic modulus and yield strength observed at the bone phase, mimicking that at the native ligament-bone junction [60]. These encouraging findings clearly demonstrate that a biomimetic stratified multi-phased scaffold system that exhibits spatial control over the phase-relevant cell heterogeneity can lead to the regeneration of complex tissues, as well as a fibrocartilage-like interface, simultaneously on a single scaffold in vivo.

In addition to the stratified scaffold design, there has been a serious shift towards designing scaffolds with a gradient of properties to ensure continuous transition in composition, structural organization, and cellular heterogeneity aiming to achieve a linear gradient in mechanical properties. For example, Subramony et al. developed a five-phased bone-interface-ligament-interface-bone polycaprolactone-PLGA/hydroxyapatite (PCL-PLGA/HA) nanofiber gradient scaffold for ACL reconstructions [68]. To form a continuous five-phased construct, a blend of PCL-PLGA was electrospun to produce aligned nanofibers at the middle of the construct for ligament regeneration. For bone regeneration, a blend of HA nanoparticles added into a solution of PCL-PLGA was electrospun at either end of the construct to produce an osteoconductive phase. For the interface regeneration, prefabricated bi-phasic nanofiber-based collars consisting of mineralized and non-mineralized regions were placed at the interface of the ligamentous and bony regions of the construct. MSCs were seeded in every junction along the graft and cultured for both in vitro and in vivo evaluations. In vitro evaluations revealed that MSCs upregulated into fibroblasts, fibro-chondrocytes, and osteoblasts specific markers on the ligament, interface, and bone phases, respectively. In vivo evaluation of the synthetic ACL scaffold showed that the nanofiber-based graft was well-tolerated, with minimal inflammatory response, and reduced the duration of the reconstruction procedure, accelerating bone formation at the mineralized region, production of a proteoglycans (GAG)–containing tissue at the interface region, and most importantly, the formation of a multi-tissue, structurally integrated ligament-bone junction. These findings highlight the potential of gradient multi-phased scaffolds in promoting ligament-bone junction regeneration, due to the continuity between the multiple phases along the graft, which facilitates enhanced cell-cell interactions as well as mechanical load transition.

Taking the mineral gradient distribution across the calcified fibrocartilage interface into account, different groups have utilized the concept of introducing a gradient of minerals or chemical cues, such as growth factors, to induce the formation

of graded calcified matrix, mimicking that found at the native ligament-bone junction. In a study done by Samavedi et al., osteogenic differentiation of stem cells seeded on polymeric composition and mineral content graded coaxial electrospun PCL fibrous scaffold was guided in a gradient-dependent manner [57, 74]. In another study done by Phillips et al., fibroblasts seeded on an electrospun collagen scaffold with a compositional gradient of retroviral coating for osteogenic transcription factor-2 (RUNX2) produced a gradient of mineralized matrix both in vitro and in vivo [75].

Considering the scaffold physical properties such as pore size, Oh et al. fabricated a PCL scaffold with different pore size gradients for ligament-bone interface regeneration via a centrifugation method [62]. The scaffold exhibits different pore size gradients along the three regions, starting from 405 μm at the bony region, with a gradual decrease to 186 μm as transitioned to the ligament region. Osteoblasts, chondrocytes, and fibroblasts were seeded in the three graft regions, respectively. Cell counting was performed along the graft, and it was found that both osteoblasts and chondrocytes showed increased cell number at the regions with pore size of 380–405 μm, while fibroblasts were more localized at areas with pore size of 186–200 μm. These findings suggest that different pore sizes can strongly affect cell behaviors such as proliferation and cell fate. Thus, providing the appropriate gradient in pore size may act as a useful tool that can guide cell differentiation and proliferation during ligament-bone interface regeneration [62].

These results demonstrate the high potential of engineering tissue-tissue interfaces by utilizing gradient multi-phased scaffold design. Gradient scaffolds exhibit continuity in the structure, which in turn can lead to improved gradual, continuous mechanical transition, cellular interactions, and gradient in mineralization across the ligament-bone junction. The physical and chemical gradual transition demonstrated in the gradient scaffold can stimulate stem cell differentiation [62]. For example, it was shown that the fate of MSCs is highly sensitive to the matrix physical properties, and they can differentiate into muscle, fibroblasts, or bone simply by changing the stiffness of the substrate [76]. In addition, pore size gradual distribution has been shown to have a large impact on guiding cell differentiation and proliferation during ligament-bone interface regeneration [62]. Gradient scaffolds are challenging to fabricate, due to the gradual transition in properties found along the scaffold length, which may limit gradation in fabrication from the nano-scale to the micro-scale found in the native ligament-bone junction, respectively. Although both stratified and gradient scaffold designs seem to overcome most drawbacks associated with complex ligament-bone interface regeneration, it is strenuous to conclude which strategy or design is best for this application. Further studies that systematically investigate and compare stratified and gradient scaffolds are needed in order to determine whether both or either is optimal for this type of regeneration. Growth factors for bone (e.g., bone morphogenetic portion-2 (BMP-2), platelet-derived growth factor (PDGF), transforming growth factor-β (TGF-β), endothelial growth factor (EGF), vascular endothelial growth factor (VEGF), insulin-like growth factor-1 (IGF-1), basic fibroblast growth factor (bFGF), and hepatocyte growth factor (HGF)) [77–80] and ligament (e.g., IGF-I, TGF-β, VEGF, bFGF, epidermal growth factor (EGF), and PDGF) [81–90], as well as biomolecules for bone (e.g., simvastatin, bisphosphonate, FTY720, purmorphamine, SVAK-12, lovastatin, rosuvastatin, helioxanthin derivative (TH), *N*-acetyl cysteine, oxysterols, and rolipram) [91–101] and ligament (e.g., collagens, Wnts, and MMPs) [102], can all be incorporated into the scaffold design as they have shown to promote the maintenance of heterotypic cell populations relevant along ligament-bone tissue interface during the regeneration process.

Tendon-Bone Interface

Tendon-Interface-Bone Structure and Function

Tendon transitions into bone through a fibrocartilage interface at the bone-tendon junction (BTJ). This fibrocartilage region is further divided intro mineralized and non-mineralized fibrocartilage zones [17]. At the non-mineralized fibrocartilage, ovoid chondrocytes are found entrapped in collagen II proteoglycan-rich matrix. At the mineralized fibrocartilage region, heterotrophic chondrocytes are found entrapped in collagen type X calcified matrix. At the bony region, referred to as the "subchondral bone," osteoblasts, osteoclasts, and osteocytes are found embedded into a mineralized collagen type I matrix. From a mechanical standpoint, the fibrocartilage interface is half as stiff as the tendon, while bone is two orders in magnitude stiffer than tendon. Under applied compression, the tendon-bone interface gradually decreases mechanical loads as they progress from tendon to bone. This mechanical synchrony presented at the tendon-interface-bone junction minimizes the formation of high-stress concentration and supports gradual load transfer from soft tissue to bone. Similar to the ligament-interface-bone junction, the cellular heterogeneity found along the tendon-interface-bone junction is a key role in permitting gradual transition of mechanical load between tendon and bone, which decreases the concentration of stress formation at the interface site [21, 22]. Furthermore, due to the similarities between tendon-bone and ligament-bone interfaces, their mechanism of development and regeneration is also similar as discussed in a previous section ("Current Understanding of the Mechanism Underlying Tendon/Ligament-Bone Interface Development and/or Regeneration").

Current Clinical Treatment for Tendon-Bone Interface Injuries

Rotator cuff tear is considered as one of the most common tendon injuries that requires an immediate medical intervention upon injury due to the poor self-healing potential. Distinct from treatment strategies followed for ligament restoration, which mainly focus on the restoration of the ligament, tendon injuries are clinically managed by re-attaching the tendon to bone via mechanical means [51, 103]. Restoration of the native tendon-bone function is challenging, and tendon postoperative detachment remains a primary reason for surgical failure [103]. Although tendon-based grafts can to certain extents restore the physiological range of motion and joint function through the mechanical fixation methods, they do not result in adequate graft integration and can result in the formation of a scar tissue at the insertion site that lacks all biological and mechanical functions of the native fibrocartilage tissue [103].

Bioinspired Scaffold Designs for Tendon-Bone Interface Regeneration

In order to address this challenge, the feasibility of integrating tendon graft to bone and facilitating the regeneration of fibrocartilage interface has been evaluated by several groups (summarized in Table 2). Most works reviewed here have employed electrospinning technique over other techniques to produce scaffolds for tendon-bone interface regeneration for several reasons. (1) The biomimetic potential of these fibrous scaffolds renders them ideal for orthopedic tissue engineering. (2) Porosity, permeability, and fiber diameter, as well as morphology, can be easily modulated during the fabrication process to resemble the native tendon ECM [116]. (3) Both randomly aligned and aligned nanofiber scaffolds can be produced by varying the electrospinning process and can be used to guide cellular response. (4) In addition, a continuous structural and compositional gradient can be achieved on nanofiber substrates using a variety of approaches [117]. Thus, the unique properties of electrospun nanofibers make them ideal for this type of application.

One of the early attempts towards the repair of rotator cuff tears using electrospun scaffolds was done by Taylor et al. [118]. In this study, randomly aligned PLGA electrospun scaffold was developed and tested both in vitro and in vivo. It was hypothesized that nanostructured resorbable polymeric scaffold can result in the production of a matrix with cellular and biomechanical properties suitable to provide initial strength with an enhanced rate of regenerative repair. In vitro evaluations showed that the scaffold supported the attachment, viability, and proliferation of patellar tendon cells for 28 days. In addition, the scaffold's mechanical properties were evaluated with and without cells, resulting in greater tensile strain when cells were cultured on the scaffold. In vivo evaluation of the electrospun scaffold in a rat rotator cuff model revealed a functional restoration of the torn tendon. These findings indicate the feasibility and potential of electrospun nanofiber scaffolds for the repair and regeneration of the tendon tissue.

To examine whether the nanofiber orientation can affect the cellular response, Moffat et al. developed PLGA nanofiber-based scaffolds and in vitro evaluated their potential for rotator cuff repair [104]. The effect of fibroblasts attachment, alignment, and gene expression has been tested as a function of nanofiber organization (aligned vs randomly aligned). It was found that the underlying orientation primarily guided tendon fibroblasts morphology, alignment, and gene expression. In addition, it was found that the deposition of collagen types I and III as well as mechanical properties was directly related to the underlying nanofiber orientation. These findings indicate that nanofiber organization plays a crucial role in guiding cell response, and clearly highlights the biomimetic potential of nanofibers to the native tendon tissue.

Building upon these successful nanofiber-based observations and taking into account the formation of fibrocartilage tendon-bone interface, Moffat et al. also reported the development of a biomimetic bi-phasic electrospun nanofibers scaffold with contiguous non-mineralized (phase A) and mineralized (phase B) regions that are designed to facilitate the regeneration of the tendon-bone interface. Phase A is composed of aligned PLGA nanofibers, and phase B consists of aligned PLGA-HA composite nanofibers. In vivo evaluations in rat [105] and sheep [106] rotator cuff models revealed the formation of fibrocartilage-like matrix at the insertion site of the graft. In addition, it was observed that mineral distribution was highly maintained, in which calcified fibrocartilage formed only at the HA-containing phase. Further, fibrocartilage matrix maturation and enhanced collagen organization at the tendon-bone junction were promoted by pre-seeding the bi-phasic scaffold with bone marrow–derived stem cells (BMDSCs). When comparing the findings to the single-phased PLGA or PLGA-HA, it was found that the regeneration of an organized fibrocartilage interface was achieved in the bi-phasic scaffold design. These observations indicate that mimicking the alignment and mineral distribution found along the native tendon-bone interface plays a crucial role in guiding cells to form a fibrocartilage-like matrix at the interface site therapy promoting its integration to the tendon and supporting calcified fibrocartilage formation and osteointegration.

Taking the mineral gradient distribution across the calcified fibrocartilage interface into account to enhance fibrocartilage formation, different groups have utilized the concept of introducing a gradation in minerals and protein content to induce the formation of graded calcified matrix, mimicking that found at the native TBJ. Li et al. demonstrated a coating-based method to generate a linear gradation of calcium

Table 2 Bioinspired scaffold designs utilized for regenerating tendon-bone interface

Scaffold type	Scaffold design	Material/s used	Fabrication method	Cell type/s	Growth factor/s	Animal model	Results	Ref
Bi-phasic	Electrospun graft with an aligned region for tendon regeneration, and unaligned region for graft attachment and augmentation	PLGA	Electrospinning	Human rotator cuff tendon fibroblasts	N/A	N/A	The underlying orientation primarily guided tendon fibroblasts morphology, alignment and gene expression. In addition, it was found that the deposition of collagen types I and III as well as mechanical properties were directly related to the underlying nanofibers orientation	[104]
Bi-phasic (gradient)	Electrospun graft with an aligned region for tendon regeneration and a mineralized unaligned region for bone regeneration. The graft was wrapped around a cylindrical bone core	PLGA/PLGA-HA	Electrospinning	Chondrocytes	N/A	Subcutaneous athymic rat model	Data revealed the formation of fibrocartilage-like matrix at the insertion site of the graft. In addition, it was observed that mineral distribution was highly maintained, in which calcified fibrocartilage formed only at the HA-containing phase. Further, fibrocartilage matrix maturation and enhanced collagen organization at the tendon-bone junction was promoted by pre-seeding the biphasic scaffold when compared to the acellular scaffold	[105]
Bi-phasic (gradient)	Electrospun graft with an aligned region for tendon regeneration and a mineralized unaligned region for bone regeneration.	PLGA/PLGA-HA	Electrospinning	N/A	N/A	Sheep rotator cuff model	Histological staining revealed that at weeks 4 and 16, an extracellular matrix rich in collagen was formed at the tendon-bone junction. Newly formed tissue was well organized, with parallel fibers inserting from tendon to bone in the scaffold groups when compared to the control (tendon attached with no scaffold). Positive proteoglycan staining at the tendon-bone junction in the scaffold group, and a well-organized mineralized neo-interface region was observed at week 16	[106]
Bi-phasic (gradient)	Electrospun woven synthetic-based scaffold consisting of non-mineralized and mineralized regions with a linear gradation in mineral content	PLGA-CaP or PCL-CaP	Electrospinning	MC3T3	N/A	N/A	Addition of CaP enhanced the attachment, spreading, and proliferation of MC3T3 cells. Region with the highest CaP content showed the highest level of cell density, and the region with the lowest CaP content had fewer cell densities. The Gradation in mineral distribution resulted in gradation in mechanical properties along the tendon-interface-bone junction. Increasing the concentration of	[107]

Table 2 (continued)

Scaffold type	Scaffold design	Material/s used	Fabrication method	Cell type/s	Growth factor/s	Animal model	Results	Ref
							bicarbonate ions resulted in an increase in mineral content that has improved the mechanical properties along the tendon-interface-bone junction	
Scaffold type	Scaffold design	Material/s used	Fabrication method	Cell type/s	Growth factor/s	Animal model	Results	Ref
Bi-phasic (gradient)	Electrospun highly porous scaffold, protein coated in a linear gradation fashion	Polymethylglutarimide (PMGI)- fibronectin	Electrospinning	NIH 3T3	N/A	N/A	Cell response on the fiber matrix depends strongly on the protein concentration. Enhanced cellular response was observed on the protein-coated scaffold when compared to non-coated scaffold.	[108]
Bi-phasic (gradient)	Osteogenic and chondrogenic growth factors incorporated in a natural-based graft gradually. This is achieved by increasing the osteogenic factor content from the center of the scaffold towards the direction of the bone, while simultaneously decreasing chondrogenic factor content in a gradation fashion, where the highest content of osteogenic factor was added at the bony region and the chondrogenic factor at the interface region, respectively	Silk	Knitting technique	MSCs	BMP-2, IGF-I	N/A	Culturing MSCs on the growth factors gradient substrate in a subchondral medium resulted in gradual increase in calcium and GAG deposition and an increase in collagen types I, II, and X gene transcription at the bony and interface regions, respectively. Further results revealed that the gradations achieved closely resembled the transition from unmineralized fibrocartilage to mineralized fibrocartilage to bone, mimicking those found at the native tissue.	[109]
Bi-phasic (gradient)	Porous synthetic-based membrane incorporated dual growth factors for accelerated tendon-bone healing.	PCL	Immersion/precipitation method	N/A	PDGF-BB, BMP-2	Rat patellar tendon avulsion model	Immobilization of both factors using "heparin-intermediated interactions" on the PCL membrane resulted in a minimal burst release in addition to a sustained and controlled release with up to 80% total release after 5 weeks. In vivo evaluations revealed that both PDGF-BB/BMP-2 dual release from the PCL membrane accelerated the regeneration of tendon-interface-bone, respectively, due to the continuous release of both factors	[110]
Scaffold type	Scaffold design	Material/s used	Fabrication method	Cell type/s	Growth factor/s	Animal model	Results	Ref
Bi-phasic (gradient)	Dual-layer organic/inorganic flexible bipolar electrospun membrane (BFM) consisting of two regions, a non-mineralized region for non-mineralized fibrocartilage	PLA	Electrospinning	N/A	N/A	Rabbit rotator cuff tear model, and rotator cuff repair	In vivo data showed that BFM significantly increased the area of glycosaminoglycan staining at the tendon–bone interface and improved collagen organization, with induced bone formation and	[111]

Table 2 (continued)

Scaffold type	Scaffold design	Material/s used	Fabrication method	Cell type/s	Growth factor/s	Animal model	Results	Ref
	regeneration, and a mineralized region for mineralized fibrocartilage regeneration for enhanced tendon-to-bone integration of enthesis						fibrillogenesis, when compared to the simple fibrous membrane (SFM) of PLA. The BFM group had also a greater ultimate load-to-failure and stiffness than the SFM group at 12 weeks after surgery when compared to the other group	
Bi-phasic (stratified)	Aligned natural-based electrospun graft for tendon-bone healing	Keratin	Electrospinning	hTCs, and MSCs secretome	N/A	Rat chronic rotator cuff tear model	The hMSCs secretome increased hTCs viability and density in vitro. In vivo, a significant improvement of the tendon maturing score was observed in the STC/hMSC/CM group (15.6 ± 1.08) compared with the MRCT group (11.0 ± 1.38; $P < 0.05$). Biomechanical tests revealed a significant increase in the total elongation to rupture (STC/hMSC/CM, 11.99 ± 3.30 mm; scaffold-only, 9.89 ± 3.47 mm; MRCT, 5.86 ± 3.16 mm; $P < 0.05$) as well as a lower stiffness (STC/hMSC/CM, 6.25 ± 1.74 N/mm; scaffold-only, 6.72 ± 1.28 N/mm; MRCT, 11.54 ± 2.99 N/mm; $P < 0.01$)	[112]
Bi-phasic (stratified)	The graft consists of two regions with different pore alignments, anisotropic at the tendon side and isotropic at the bone side	Silk Fibroin	Directional freezing	hADMSCs	N/A	N/A	Bi-phasic scaffold supported cell attachment and influenced cell organization depending on pore alignment. In addition, the gene expression of tendon/ligament, enthesis, and cartilage markers significantly changed depending on pore alignment in each region of the scaffold	[113]
Scaffold type	Scaffold design	Material/s used	Fabrication method	Cell type/s	Growth factor/s	Animal model	Results	Ref
Tri-phasic (gradient)	A hierarchically structured scaffold composed of three regions with distinct functions: an array of channels to guide the in-growth of cells and aligned deposition of the fibers, as well as integration of the scaffold with the tendon side, a region with a gradient in mineral composition for interface regeneration, and a mineralized inverse opal region to promote osteointegration.	PLGA-HA/Gelatin	Custom fabrication method	ADSCs	N/A	N/A	Cell culture experiments confirmed that ADSCs were able to infiltrate and proliferate through the entire thickness of the scaffold without compromised cell viability. The seeded stem cells exhibited directed differentiation into tenocytes and osteoblasts along the mineral gradient as a response to the gradient in young's modulus	[114]
			3-D printing	MSCs	N/A			[115]

Table 2 (continued)

Scaffold type	Scaffold design	Material/s used	Fabrication method	Cell type/s	Growth factor/s	Animal model	Results	Ref
Tri-phasic (gradient)	A hollow cylindrical shape, 3-D printed scaffold for tendon-bone regeneration	PCL, PLGA and β-TCP				Rabbit ACL reconstruction model	Histological analysis showed that a smooth bone-to-tendon transition through broad fibrocartilage formation was identified in the treatment group, and the interface zone showed abundant type II collagen production on immunohistochemical staining. Bone-tendon healing histologic scores were significantly higher in the treatment group than in the control group (without cell seeding) at all time points. μCT analysis at 12 weeks showed smaller tibial (control, 9.4 ± 0.9 mm^2; treatment, 5.8 ± 2.9 mm^2; $P = 0.044$) and femoral (control, 9.6 ± 2.9 mm^2; treatment, 6.0 ± 1.0 mm^2; $P = 0.03$) bone-tunnel areas in the treated group than in the control group	

N/A, not available

phosphate on a nonwoven mat of a polymeric electrospun nanofiber by varying the incubation time of the scaffolds in a concentrated simulated body fluid (SBF). The gradation in mineral distribution resulted in gradation in mechanical properties along the TBJ [107]. To further improve the mechanical properties, the soaking solution was optimized by increasing the concentration of bicarbonate ions, which resulted in an increase in mineral deposition that improved the mechanical properties along the TBJ [119]. In order to evaluate the ability of the pre-coated scaffold to induce graded osteogenesis, adipose-derived MSCs were seeded along the scaffold resulting in more extensive staining of osteogenic markers that was observed in areas with higher mineral content [120]. The effect of the mineral gradient distribution on fibrocartilage interface formation was also evaluated by Harley et al. utilizing a unique approach [121]. Herein, a biphasic collagen-glycosaminoglycan-based (CG) scaffold with different mineral contents along the scaffold's length mimicking the structural and compositional features of the native TBJ was fabricated for tendon-bone interface regeneration. To fabricate the scaffold, a degassed suspension of CG was placed at the bottom of a cylindrical mold (6 mm diameter, 15 mm deep) until half of the mold was filled. The other top half of the mold was then filled with CG/CaP suspension, which was carefully layered on top of the CG suspension. Both suspensions were then allowed to partially interdiffuse for 20 min before freeze-drying to promote continuity of collagen fibers across the interface, which resulted in a continuous tendon-bone scaffold with divergent mineral content, where the highest mineral content is localized at the bony phase, and decreases as transitioned to the tendinous phase mimicking those found at the native TBJ. Micro-computed tomography (μCT) and energy-dispersive X-ray (EDX) analysis confirmed extensive localization of the mineral mostly at the bony phase of the scaffold, but minimal localization at the interface, with no localization observed at the tendinous phase [122]. To evaluate the cellular response to the mineralized gradient scaffold, MSCs were pre-seeded along the scaffold length for 6 weeks in the absence of a differentiation medium, resulting in extensive osteogenic, chondrogenic, and tenogenic gene expression at the bony, interface, and tendinous regions, respectively. To evaluate the effect of protein gradient distribution, Shi et al. evaluated the effect of fibronectin protein gradation on polymeric electrospun nanofiber scaffold for the formation of tendon-bone fibrocartilage interface, which found to exhibit control over density and morphology of cultured NIH 3T3 fibroblasts [108]. These findings suggest that gradation in mineral or/and protein content along the bone-interface-tendon graft may result in spatial control over osteogenesis and tenogenesis, and may promote the formation of fibrocartilage interface in between.

To evaluate the potential of growth factors in restoring the native tendon-bone interface, several groups have introduced different growth factors such as PDGF, BMP-2, IGF-I, bFGF, and TGF-β into their scaffold designs. Lee et al. estimated the feasibility of gradually immobilizing both PDGF-BB and BMP-2 in an asymmetrically porous PCL membrane as a potential strategy for effective regeneration of tendon-bone interface. Both growth factors were immobilized using "heparin-intermediated interactions," which resulted in a minimal burst release in addition to a sustained and controlled release with up to 80% total release after 5 weeks. In vivo evaluation in rat patellar tendon avulsion model revealed that both PDGF-BB/BMP-2 dual releases from the PCL membrane accelerated the regeneration of tendon-bone interface, respectively, due to the continuous release of both factors [110].

In a different study, both BMP-2 and IGF-I were used by absorbing different concentrations of BMP-2 and IGF-I along a tendon-bone silk construct [109]. This was achieved by increasing BMP-2 content from the center of the scaffold towards the direction of the bone, while simultaneously decreasing IGF-I content in a gradient manner, where the highest content of BMP-2 was added at the bony region, and IGF-I at the interface region, respectively. Culturing MSCs on the substrate with growth factors gradient in a subchondral medium resulted in a gradual increase in calcium and GAG deposition and an increase in collagen types I, II, and X gene transcription at the bony and interface regions, respectively. Further results revealed that the gradient scaffold closely resembled the transition from unmineralized fibrocartilage to mineralized fibrocartilage to bone, mimicking those found at the native tissue junction. These results demonstrate the feasibility and the potential of gradual immobilization of growth factors and the dual delivery of both factors from tendon-bone grafts for the regeneration and the restoration of the complex tendon-bone interface.

Muscle-Tendon Interface

Muscle-Interface-Tendon Structure and Function

Tendon is a highly organized connective tissue that connects muscles to bone through a characteristic fibrocartilage interface at either end, which plays an important role in gradually transmitting force between muscle and bone [123]. Three specialized regions are characterized along the muscle-tendon-bone junction: the myotendinous junction (MTJ), the tendon proper with the region where tendons change direction by wrapping around bony pulleys, and the bone-tendon junction BTJ [124]. The MTJ is further divided into muscle and tendon regions overlapping through an interface in between. At the muscle region, myoblasts are found entrapped in collagen type IV. At the interface, muscle and tendon meet, creating a network of overlapping muscles and tendon tissues with a greater surface area for adhesion between them. Several adhesion

proteins are found at the interface ECM that include, integrin, laminin, vinculin, paxillin, and talin in addition to the ECM-specific proteins for both tissues, muscles and tendons [125–129]. At the tendon tissue, tendon fibroblasts are found entrapped in collagen type I matrix [130].

Four separate ultrastructural domains are found along the MTJ connecting the actin filaments of the terminal sarcomere with the collagen fibers of the tendon. (1) "*the internal lamina*," composed of actin filaments and associated crosslinking structures; (2) "*the connecting domain*," which connects the internal lamina to the external lamina; (3) "*the lamina densa of the external lamina*," with a structure similar to other laminae densa; and (4) "*the matrix*," found in the space between lamina densa and the collagen fibers [131].

Mechanically, tendon is stiffer than muscle, and this is to allow for adequate transfer of forces from muscle to bone without undergoing significant deformation at the tendon. Structurally, tendon fibers are merged to the muscle ECM. Some muscles have tendons that are significantly shorter than the length of the muscle fibers, while other muscles have tendons that are several folds longer than the length of the muscle fibers. Thus, the greater the length of the tendon compared with the muscle, the greater the muscle will need to contract in order to move a given distance or to achieve a given velocity [132]. This implies that the relative length of the tendon fibers to muscle fibers at the MTJ can differ from one MTJ to another and thus, this variance should be considered when designing a scaffold for MTJ regeneration, depending on the MTJ targeted for repair.

Current Understanding of the Mechanism Underlying Muscle-Tendon Interface Development and/or Regeneration

Although the exact mechanism of MTJ development is not well understood, studies suggest that the interaction between tenocytes and myotubes is an essential process that leads to the formation of a specialized muscle-tendon interface [133]. In fact, the development of MTJ is influenced by some factors that are essential to establish a functional muscle-tendon interface including interactions within muscle and tendon cells and interactions between the future forming muscle and tendon tissues in addition to some functional and structural interactions between tenocytes and myocytes at the site of the future MTJ [133]. These interactions take place gradually until a complete and functional MTJ is formed. First, cells within tendon interact forming a rich collagen matrix. Muscle cell interactions result in the formation of well-developed muscle tissue that consists of myofibers. Myofibers then apply a lateral force to the tendon by the muscle contraction. In response to this contractile force applied to the tendon, tenocytes and the tendon's ECM components such as collagen fibers align themselves in the direction of the applied force. This allows for direct contact between tendon and muscle through long cytoplasmic processes. This direct contact enables the tapered ends of the muscle myofibers to embed into the ECM of the tendon, forming a well-developed MTJ through the creation of a network of overlapping muscle and tendon tissues with a greater surface area for adhesion [130, 133].

In an attempt to address the mechanism of the MTJ's development, Larkin et al. developed an in vitro model of three-dimensional (3-D) skeletal muscle-tendon constructs based on the hypothesis that an in vitro 3-D engineered skeletal muscle-tendon constructs would develop MTJs resembling those found during fetal development in vivo [134]. To validate the hypothesis, MTJ structures in vivo have been compared with those developed in 3-D skeletal muscle constructs co-cultured with engineered self-organized tendon constructs (SOT) or segments of adult (ART) or fetal rat tail (FRT) by means of electron microscopy [134]. In vitro evaluations revealed that some of the myofibers of the engineered 3-D skeletal muscle-FRT and SOT constructs only displayed emerging finger-like sarcolemmal projections surrounded by collagen fibers, which structurally resemble fetal MTJs in vivo. In addition, a complete MTJ was developed on the muscle-FRT constructs. These findings suggest that the muscle-FRT construct model could be used for studies of developmental mechanisms involved in the establishment of interfaces among all four muscular-skeletal tissues: muscle, tendon, and cartilage/bone, including the two tissue-specific cellular interactions at the insertion site.

Current Clinical Treatment for Muscle-Tendon Interface Injuries

Muscle-tendon interface regeneration is another critical research area in addition to tendon-bone interface regeneration. As tendon connects muscle to bone, the MTJ connects muscle to tendon and acts as a bridge to distribute mechanical loads between muscles and bones [135]. Therefore, any injury at the muscle-tendon junction will result in failure in mechanical load distribution that can cause movement restrictions and low quality of life to the injured individual [135]. Current clinical treatments include conservation or surgical approaches. In conservation treatment, the patient is normally asked to rest to relieve the pain or is given injections of a variety of drugs, including corticosteroids and physiotherapy. Due to the limited self-healing capacity of tendons, this type of treatment can result in prolonged treatment time, recurrent injury, weakness in the affected site, and thus partial loss of function that may necessitate extensive and intensive future rehabilitation [136, 137].

Surgical intervention includes the use of autografts and allograft to treat tendon injuries. However, the high cost, pain, and the donor site morbidity associated with harvesting autograft, as well as the limited availability, poor biocompatibility,

and poor integration of allografts to the host tissues, limit their clinical use in most cases for this particular application [138].

Mechanical stimulation of the cells is known to promote cell proliferation and differentiation and has been utilized as another treatment strategy to treat muscle-tendon injuries. During the treatment, mechanical stimuli are applied to the injured site which stimulate cells to secrete biochemical signals that aid in the healing process [139]. Although this treatment has shown signs of healing in some cases, the optimal treatment parameters such as treatment duration, frequency, magnitude, and type of mechanical stimulation applied to the tendon are yet to be identified and can vary from one patient to another, resulting in inconsistent outcomes between patients [140, 141]. Limitations associated with the current clinically used treatments clearly highlight the need for more functional and integrative methods that mostly focus on effectively regenerating these tissues rather than repairing them.

Bioinspired Scaffold Designs for Muscle-Tendon Interface Regeneration

To date, relatively very few studies have explored the feasibility to muscle-tendon interface regeneration comparing to the tendon-bone interface. This may be due to the fact that the majority of tendon injuries occur at either the tendon proper or the tendon-bone insertion, which limits the number of trials in this area [142].

Engineering approaches for muscle-tendon interface regeneration (summarized in Table 3) may include the use of scaffold-based techniques or may be associated with scaffoldless fabrication methods. Scaffold-based approaches include the use of composite, stratified, and gradient scaffolds, in which the native tissue can effectively be stimulated and mimicked. On the other hand, scaffoldless approaches largely rely on the concept of cellular self-assembly or self-organization for tissue formation or repair without the use of an exogenous substrate [146].

An ideal scaffold design for muscle-tendon interface repair should mimic every single aspect found at the native tissue for successful restoration of the muscle-tendon junction. The engineered scaffold should consist of distinct multiple phases with different mechanical properties with the ability to withstand mechanical load values near that undergone by the native tissue junction. In addition, the scaffold should structurally and compositionally mimic the native muscle-interface-tendon junction [146].

The first successful fabrication of multiphasic muscle-tendon graft with functional MTJ was adopted by Larkin et al. From a heterogeneous muscle "sarcolemma" and tendon "fibroblasts" isolations, a scaffoldless substrate has been fabricated by co-culturing both cell types. Specifically, cylindrical scaffoldless multiphasic tissue construct was created with robust interfaces. The contractile and structural characteristics of the muscle constructs co-cultured with (1) engineered self-organized tendon constructs or (2) segments of adult or (3) fetal rat-tail tendon have been evaluated in vitro. In addition, the construct diameter (1 mm) and maximum isometric force (microN) were measured, and specific force in (kPa) was determined. In vitro evaluations revealed that the neo-interface region exhibited upregulated expression of muscle-tendon junction-specific paxillin, and has been able to maintain tensile loading at super-physiologic strain rates [134]. Furthermore, when extended to the point of rupture, they failed at the mid-substance of the engineered muscle, with the muscle-tendon interface intact. When implanted in vivo, it resulted in complete maturation and integration to the native tissue [133]. In vivo implantation also resulted in an increase in force production, which in turns strengthened the MTJ. This successful initial step towards the regeneration of the muscle-interface-tendon junction clearly outlines the feasibility of engineering an MTJ substrate.

Larkin et al. have further investigated another possibility of restoring the MTJ by developing an in vitro model of 3-D skeletal muscle-tendon constructs to address mechanisms of the MTJ development. In this study, it was hypothesized that an in vitro 3-D engineered skeletal muscle-tendon constructs would develop MTJs ultrastructurally resembling those found during fetal development in vivo [133]. The native MTJ tissue structure was compared with those developed in the 3-D skeletal muscle constructs co-cultured with engineered SOT, or ART or FRT by electron microscopy. In vitro evaluations revealed that some of the myofibers of the engineered 3-D skeletal muscle-FRT and SOT constructs only displayed emerging finger-like sarcolemma projections surrounded by collagen fibers, which structurally resemble the fetal MTJ tissue. In addition, a complete muscle-interface-tendon junction was developed on the muscle-FRT constructs. These findings suggest that the muscle-FRT construct model could be used for studying the mechanisms of MTJ development as well as other developmental studies involved in the establishment of interfaces among muscular-skeletal tissues: muscle, tendon, and cartilage/bone.

Recently, Ladd et al. developed a tri-phasic polycarbonate-collagen (PC-collagen) and poly(lactic acid)-collagen (PLA-collagen) co-electrospun nanofibers scaffold onto opposite ends of a mandrel to create a scaffold with three regions for engineering muscle-tendon junction [144]. In vitro evaluation demonstrated that the scaffold exhibited regional variations in mechanical properties with moduli from 4.490 to 27.62 MPa, similar to the native muscle-tendon junction and generally withstood cyclic testing. In addition, further results revealed that the scaffold facilitated both myoblast and fibroblast attachment at the relevant-cell regions.

To this end, muscle-tendon interface regeneration is a critical research area for integrative tendon repair that has not been explored enough yet. Further studies in this area are

Table 3 Bioinspired scaffold designs utilized for regenerating muscle-tendon interface

Scaffold type	Scaffold design	Material/s used	Fabrication method	Cell type/s	Growth factor/s	Animal model	Results	Ref
Bi-phasic (scaffoldless)	Scaffoldless substrate fabricated by co-culturing two different cell types	N/A	Self-assembly/ self--organization	Muscle sarcolemma and tendon fibroblasts	N/A	Rat model	In vitro evaluations revealed that the neo-interface region exhibited upregulated expression of muscle-tendon junction-specific paxillin, with the formation of an intact muscle-tendon interface. In vivo evaluation revealed a complete maturation and integration to the native tissue as well as an increase in force production.	[133]
Bi-phasic (decellularized)	Decellularized porcine Achilles tendon myotendinous junction, with well-preserved native bi-phasic hierarchical structure, biological composition, and excellent mechanical properties for muscle regeneration	N/A	Decellularization technology	Muscle satellite cells	N/A	Subcutaneous rat model	In vitro evaluation revealed that the decellularized construct supports muscle satellite cells attachment, proliferation and infiltration throughout, as well as the differentiation into myofiber-like cells. In vivo results demonstrated the neo-formation of myofibers along the construct.	[143]
Tri-phasic (gradient)	Electrospun synthetic and natural-based scaffold consisting of three regions for muscle, interface and tendon regeneration, respectively.	PCL/Collagen or PLLA/Collagen	Electrospinning	NIH 3T3	N/A	N/A	In vitro evaluation demonstrated that the scaffold exhibited regional variations in mechanical properties with moduli from 4.490–27.62 MPa, similar to the native muscle-tendon junction and generally withstood cyclic testing. Further results revealed that the scaffold facilitated both myoblasts and fibroblasts attachment at the relevant-cell regions.	[144]
Tri-phasic (gradient)	3-D printed graft consisting of three regions, all regions were co-printed with cell-laden hydrogel based bioink with different polymers and different cell types to mimic the different aspects of the native muscle-tendon junction.	Polyurethane (PU) (muscle phase), and PCL (tendon phase)	3-D printing	C2C12 (for muscle regeneration), and NIH 3 T3 (for tendon regeneration)	N/A	N/A	The final construct was elastic on the PU-C2C12 muscle side ($E = 0.39 \pm 0.05$ MPa), stiff on the PCL-NIH/3 T3 tendon side ($E = 46.67 \pm 2.67$ MPa) and intermediate in the interface region ($E = 1.03 \pm 0.14$ MPa). The construct supported cell viability after 1 and 7 days post-printing, as well as initial tissue development and differentiation.	[145]

required to overcome many limitations associated with MTJ regeneration. The addition of growth factors such as IGF-I and II, TGF-β, VEGF, bFGF, EGF, and PDGF [147, 148] into the scaffold design may enhance the regenerative potential of the MTJ and/or overcome some of the current limitations.

Cartilage-Bone Interface

Cartilage-Interface-Bone Structure and Function

Cartilage Zone Structure and Function

Osteochondral (OC) is a uniquely structured tissue that is comprised of articular cartilage, the subchondral bone, and the central cartilage-bone interface [149]. This unique hierarchical structure plays an important role in maintaining the knee homeostasis as well as providing the synchrony in physiological movements. The articular cartilage is further divided into three distinguishable well-organized zones from top to bottom [150]. The top zone is the superficial or tangential zone, occupying 10–20% of the articular cartilage [151]. The middle zone occupies the following 40–60% of the articular cartilage, and the remaining thickness is occupied by the deep zone and the calcified cartilage which are believed to be 30% of the total articular cartilage thickness.

Cells within the superficial zone or "articulating surface" are known to secrete special types of proteins that facilitate the wear and frictional properties of the tissue during movement [152]. The middle zone, the largest zone, has the most abundant content of GAG with the least number of cells. This zone is known for its obliquely oriented collagen fibrils, which inherit its high compressive modulus that allows for recovery from impacts undergone by the articular surface [153, 154]. In the deep zone, where the fibrils are anchored to the underlying subchondral bone, cells and collagen fibrils are oriented perpendicularly to the articular cartilage's surface [155]. This zone is known for its high compressive modulus, less GAG content comparing to the middle zone, and less cellular content comparing to the previous two zones [156]. The GAG content of the two last layers enables the extracellular matrix to withstand high compressive forces. At the bottom of the deep zone, a thin layer known as the "tidemark" or "wavy tidemark," marks the interface between the last calcified cartilage zone to the subchondral bone. This layer is important, as it separates between the calcified and uncalcified cartilage, and is responsible for regulating the activities of chondrocytes in both regions. In addition, this last layer is known to minimize the stiffness gradient between the cartilage and subchondral bone. The cell content and the collagen fibrils are very minimal in this last layer [157].

The articular cartilage is a rich collagen tissue that is mainly composed of collagen type II. Other collagen types such as V, VI, IX, and XI are also present throughout the zonal cartilage, and play a key role in the intermolecular interactions and the modulation of type II collagen [158]. In addition, type X collagen is known to assist in the mineralization between the cartilage and underlying bone [159].

Subchondral Bone Structure and Function

The subchondral bone is the last component of the OC tissue that is located just below the interface between the zonal cartilage and the subchondral bone. It is composed of two bony zones, lamella and trabeculae. The lamella contains a large mass of bone with thickness varying between 0.2 and 0.4 mm in humans [160]. The subchondral trabecular bone supplies both the lamella and the adjacent articular cartilage with nutrition and oxygen due to its high vasculature nature [161]. The three main functions of the subchondral bone are absorption, maintaining joint shape, as well as providing the strength to the adjacent articular cartilage due to its large area and low modulus of elasticity [162].

Current Understanding of the Mechanism Underlying Cartilage-Bone Interface Development and/or Regeneration

Cell-cell interactions between the subchondral bone and the zonal cartilage are very important for the formation of the tidemark interface. The interactions between many cell types have been examined to understand their contributions in the formation of cartilage-bone interface in the OC tissue by co-culturing cells relevant to tissue types like fibroblasts, osteoblasts, and chondrocytes, or stem cells such as MSCs in biomimetic 3-D microenvironments [163, 164]. For example, Jiang et al. studied whether relevant tissue cells such as chondrocytes and osteoblasts can contribute and interact to form the interface found at the cartilage-bone junction [165]. In this study, a stratified agarose hydrogel and composite microspheres of PLGA and 45S5 BG scaffold mimicking the three distinct yet continuous regions of cartilage calcified cartilage and bone has been developed. The scaffold was developed in order to evaluate the potential of OC interface formation by co-culturing chondrocytes at the agarose hydrogel phase and osteoblast at the PLGA-BG phase. In vitro analysis showed extensive chondrogenesis and improved graft mechanical property over time. In addition, it was shown that PLGA-BG phase promoted chondrocyte mineralization, which in turn aided the formation of the interface region and bone. These results suggest that co-culturing the relevant tissue cells such as chondrocytes and osteoblasts has the potential to improve OC interface formation.

In a similar approach, Chen et al. created a stem cell–derived OC interface using an interface-specific microenvironment in a 3-D configuration via multilayered co-culturing

[166]. In this study, MSCs were encapsulated in collagen microspheres, which guided their differentiation into chondrogenic and osteogenic functional units that enabled the formation of the mediated interface. The pre-differentiated functional microsphere layers were combined to form a tri-layered scaffold with the chondrogenic microspheres on top and osteogenic microspheres at the bottom, intermediating with an undifferentiated layer of MSCs encapsulated in collagen microspheres. Culturing the tri-layered construct in a chondrogenic medium generated a continuous calcified interface with hypertrophic chondrocytes and extensive production of collagen type X. In addition, sandwiching the undifferentiated MSC with the two differentiated layers in the co-culture system resulted in enhanced integration of the three distinct phases enabling the formation of an OC-like interface. These data suggest that co-culturing differentiated and undifferentiated MSCs in an appropriate 3-D microenvironment can stimulate them and guide their fate towards the regeneration of OC interface.

Findings from these two studies suggest that both tissue-relevant cells and stem cells have the potential to interact when co-cultured in biomimetic 3-D microenvironments and form an interface-like tissue. Further studies are required in order to study the mechanism governing the heterogeneous cellular interactions of these cells for prolonged times to examine their potential to sustain the formation of the interface-like tissues.

Current Clinical Treatment for Osteochondral Defects (OCD)

Articular cartilage is a connective tissue that acts as a shock absorber and facilitates joint motion in low friction [149]. Like any other tissue, the articular cartilage is prone to lesions for many reasons, such as traumatic events, chronic repetitive microtrauma, and aging [167]. Distinct from bone, the avascular nature of articular cartilage makes it irreparable due to the consequent lack of supplementation of potentially reparative cells/bioactive factors, which makes the possibility of cartilage to self-regenerate below minimal [168]. As the cartilage lesion progresses, it extends to the underlying subchondral bone and the OCD appears. Not only diseases orienting from cartilage will result in OCD, in fact, other diseases originating from the subchondral bone can also induce OCD when the cartilage layer is reached, such as osteochondritis dissecans and osteonecrosis [169].

As a result of the OCD, the formation of fibrocartilage tissue at the defect site takes place, which only provides very poor protection to the subchondral bone [170]. The continuous movement of the individual can cause a subsequent degradation to the newly formed fibrocartilage tissue followed by degradation to the adjacent tissues, resulting in impaired joint mobility, severe pain, and low quality of life, which necessitate the clinical intervention [171, 172].

Current clinical treatments to OCD are limited by arthroscopic debridement, bone marrow stimulation techniques, the use of OC allografts, autologous chondrocyte implantation (ACI), or matrix-assisted chondrocyte implantation (MACI) [173, 174]. Although arthroscopic debridement and bone marrow stimulation techniques have shown the same positive results in treating OCD, these techniques are palliative, but not curative and have no significant benefits for larger OCDs [76].

ACI and MACI are two clinical reparative techniques that to a certain extent have overcome most of the drawbacks associated with the discussed conventional clinical treatments. ACI generally involves an arthroscopic evaluation of the defect site, followed by a biopsy collection from the same patient. The biopsy is then used to isolate autologous chondrocytes, expand them in culture, and finally seed them back onto the affected area [174]. A similar approach is followed for the MACI with a slight difference, where the chondrocytes are first seeded on a biodegradable matrix and then implanted at the affected area [174]. Although these two approaches are considered the gold standard among all the alternative clinical treatments in modern medicine, limitations are still present that include the creation of a secondary OCD during the biopsy, the multiple numbers of surgeries required, and the relatively long recovery time, as well as the slow regeneration of the defect [175].

The aforementioned clinical treatments are more focused on either palliating the pain associated with the OCD or repairing the damaged cartilage only. It has been shown in many reports that without the support from the subchondral bone, any treatment to re-establish the cartilage layer is likely to fail [176]. The cartilage and subchondral bone should be taken into account as one unit during OC regeneration, instead of being considered separately. This comes after the fact that both the zonal cartilage and the subchondral bone are tightly connected, and no matter where the disease is orienting from, the other adjacent tissues will always be affected, which will result in negative contributions to the mechanical homeostasis of the whole joint [177].

In other words, OCD leads to the degeneration of bone, cartilage, and the bone-cartilage interface. For OCD regeneration to be possible, it is essential that each of these components be taken into account as one complex synchronized unit during OC regeneration, instead of being considered separately, as the main goal for OC regeneration is to restore its biomechanical properties, besides the regeneration of the defect.

Bioinspired Scaffold Designs for Cartilage-Bone Interface Regeneration

Several scaffold designs and engineering approaches have been applied aiming to achieve an integrative and a functional regeneration to the OCD (summarized in Table 4). One of the very early engineering attempts to regenerate an OCD was

Table 4 Bioinspired scaffold designs utilized for regenerating cartilage-bone interface

Scaffold type	Scaffold design	Material/s used	Fabrication method	Cell type/s	Growth factor/s	Animal model	Results	Ref
Single-phased	Synthetic-based porous cubes as a cell carrier for OCD regeneration	PLLA	N/A	Chondrocytes	N/A	Rabbit OCD model	Both in vitro and in vivo evaluations showed extensive production of collagen type I as high as 81 ± 4%, with very minimal production of collagen type II. Although the single-phased scaffold did not show evidence for sufficient production of collagen type II, it supported the proliferation, attachment and survival of the pre-seeded chondrocytes	[178]
Single-phased	Two different types of highly porous scaffolds produced by two different fabrication methods for OCD regeneration	PEGT/PBT	CM, and 3-D FD	Chondrocytes	N/A	Subcutaneous in a nude mouse	Pore size analysis revealed that both scaffold types had variations in pore sizes, where the CM produced scaffolds had an average pore size of 182 μm, while the average pore size in the 3-D FD produced scaffolds was 525 μm. Both scaffolds supported cell proliferation and GAG production for up to 14 days with no significant difference. In vivo data showed that there was an increase in GAG production in the 3-D FD scaffolds in comparison to the CM scaffolds along with a better mechanical integrity	[179]
Singles-phased	Electrospun scaffold produced from composite polymers for OCD regeneration	Poly (vinyl alcohol)--methacrylate, and low-density chondroitin sulfate methacrylate	Electrospinning	MSCs	N/A	Subcutaneous athymic mouse model	Scaffold supports MSCs proliferation and chondrogenic differentiation with an extensive deposition of GAG, lacunae and collagen type II in vitro. In vivo evaluations for the scaffold revealed that the cellular nanofiber scaffold had a higher proteoglycan deposition than the acellular but less proteoglycan deposition than normal articular cartilage. Deposition of collagen type II was also observed in vivo in the cellular scaffold group	[180]
Single-phased (hybrid)	Cylindrical scaffolds	PLA/ACP	Thermally induced phase separation technique	N/A	bFGF	Rabbit OCD model	In vivo assessments revealed that the PLA-bFGF treated defects presented better defect regeneration when compared to the untreated group in all time points, with low amount of collagen type II and bone formation observed and a completely negative expression to aggrecan. Further data revealed that the defect treated with PLA/ACP-bFGF was completely filled with well-established cartilage, in addition	[181]

Table 4 (continued)

Scaffold type	Scaffold design	Material/s used	Fabrication method	Cell type/s	Growth factor/s	Animal model	Results	Ref
							to extensive deposition of collagen type II as well as aggrecan that was observed at 12 weeks.	
Scaffold type	Scaffold design	Material/s used	Fabrication method	Cell type/s	Growth facto-r/s	Animal model	Results	Ref
Single-phased	Natural-based hydrogel filled with cell aggregate	Fibrin	N/A	BMSCs	N/A	Rat OCD model	Fibrin gel encapsulated with high density of BMSC aggregates demonstrated a complete repair to the defect. In addition, Extensive GAG and collagen types I and II production with a moderate staining of Safranin O in the high-density aggregates group comparing to the low density and fibrin alone was observed	[156]
Single-phased	Synthetic-based scaffold with radially oriented pores through an applied unidirectional cooling for the regeneration of an OCD tissue	PLGA	Unidirectional cooling technique	BMSCs	N/A	Rabbit OCD model	The scaffold was highly porous (90%), with a compressive modulus of 4 MPa. Culturing BMSCs in vitro revealed faster migration and regular distribution of cells in throughout the scaffold with oriented pores compared with the random un-oriented scaffold. In vivo evaluations confirmed obvious interface regeneration, regular chondrocytes distribution, and lacunae in the cartilage layer. Further histological analysis confirmed the simultaneous re-generation of the cartilage and subchondral bone layers, which was not evident in the un-oriented group.	[182]
Bi-phasic (gradient)	Both scaffolds are commercially available for OCD regeneration treatment. Both scaffold consist of an upper portion for cartilage regeneration and a lower portion for bone regeneration	Collagen–GAG-CaP, and PLGA-PGA	N/A	N/A	N/A	Caprine OCD model	In vivo evaluations revealed that the collagen-GAG-CaP scaffold became stiffer and provided radical mechanical reinforce-ment after 12 weeks in comparison to the PLGA/PGA scaffolds. After 26 weeks, defects treated with collagen-GAG-CaP had significantly higher content of hyaline cPGA scaffolds/PGA scaffolds, 75–50%, respectively. In addition, the histological score in the lateral trochlear sulcus was significantly higher when treated with the collagen-GAG-CaP scaffold than PLGA/PGA scaffolds	[183]
Scaffold type	Scaffold design	Material/s used	Fabrication method	Cell type/s		Animal model	Results	Ref

Table 4 (continued)

Scaffold type	Scaffold design	Material/s used	Fabrication method	Cell type/s	Growth factor/s	Animal model	Results	Ref
					Growth facto-r/s			
Bi-phasic (stratified)	The scaffold consists of two regions, where the upper region is a natural polymer-based for cartilage regeneration, while the lower region is a synthetic and natural polymer -based for bone regeneration	Collagen, PLGA-collagen	Particulate-leaching technique	BMSCs	N/A	Beagle OCD model	Four months after implantation, it was found that cartilage and bone-like tissues were formed in the respective regions. Additional in vivo data revealed that the implant well integrate with the surrounding host tissues.	[184]
Bi-phasic (gradient)	Cylindrical scaffold consisting of two regions, where the first region is loaded with a chondrogenic factor for cartilage regeneration, while the second region is loaded with an osteogenic and chondrogenic factors for bone regeneration	PLGA, and PLGA-HA	Heat sintering	N/A	TGF-β 1, and BM-P-2	Rabbit OCD model	Great extent of cartilage and subchondral bone were achieved in the growth factors loaded groups when compared to the controls based on the gross morphology. In addition, the growth factors loaded group showed well edge integration with the host bone when compared to all the other groups after 12 weeks	[185]
Tri-phasic (gradient)	Hydrogel-based scaffold with two regions and an interface graft placed in the middle separating the two regions. The two regions exhibit different stiffness resembling those found at the native OC tissue	CAN-PAC (hydrogel), and calcium gluconate-alginate (interface graft)	Thermally reactive rapid cross-linking method	N/A	N/A	Rabbit OCD model	Stiffness variations along the hydrogel guided different cellular response. Complete regeneration of cartilage, interface and bone was evident by μCT and histological analysis in the CAN-PAC group when compared to the other group 18 weeks after implantation.	[186]
Scaffold type	Scaffold design	Material/s used	Fabrication method	Cell type/s	Growth facto-r/s	Animal model	Results	Ref
Tri-phasic (gradient)	3-D printed hydrogel-based scaffold with three regions, a gel region, shear-thinning region, and a scaffold forming region; for OCD regeneration.	PNAGA, and β-TCP particles	3-D printing	hBMSCs	TGF-β1	Rat OCD model	The gradient 3-D printed growth factors loaded hydrogel scaffold facilitates the attachment, spreading, and chondrogenic and osteogenic differentiation of hBMSCs in vitro. In vivo experiments revealed that the 3-D printed gradient hydrogel scaffold significantly accelerated simultaneous re-generation of cartilage and subchondral bone	[187]
Tri-phasic (gradient)	Hierarchically structured scaffold with three regions, a top region for cartilage regeneration, a middle region and slightly mineralized for the interface regeneration, and a lower but highly mineralized region for bone regeneration.	PCL, and PCL-HA	Selective laser sintering (SLS) technique	MSCs	N/A	Rabbit OCD model	The gradient scaffold showed excellent biocompatibility, as it supported cell adhesion and proliferation in vitro. In vivo data revealed that the gradient scaffold was able to induce articular cartilage formation by accelerating the early subchondral bone regeneration, and the newly formed tissues	[188]

Table 4 (continued)

Scaffold type	Scaffold design	Material/s used	Fabrication method	Cell type/s	Growth factor/s	Animal model	Results	Ref
							could well integrate with the native tissues	

N/A, not available

adopted by Chu et al. In this study, commercially available PLA cubes were used to fabricate a single-phased OC scaffold. Peri-chondrocytes were derived from the cartilage of New Zealand white rabbits and used to pre-seed the scaffolds prior to in vitro and in vivo evaluations [178]. Both in vitro and in vivo evaluations showed an extensive production of collagen type I as high as 81 ± 4%, with very minimal production of collagen type II. Although the single-phased scaffold did not show evidence for sufficient production of collagen type II, it supported the proliferation, attachment, and survival of the pre-seeded peri-chondrocyte cells.

In a different attempt, Malda et al. evaluated the effect of the scaffold's fabrication techniques on the OC regeneration based on the hypothesis that the scaffold design can highly affect the regeneration of the OC tissue [179]. In this study, two different fabrication techniques, compression molding, and 3-D fiber deposition were used in order to fabricate a single-phased scaffold using the biodegradable poly(ethylene glycol) terephthalate/poly(butylene terephthalate) (PEGT/PBT). Pore size analysis revealed that there was a significant pore size variation between the two scaffold designs, where the compression molding scaffolds had an average pore size of 182 μm, while the 3-D fiber deposition scaffolds had an average pore size of 525 μm. To further validate the hypothesis, both scaffolds were pre-seeded with chondrocytes and in vitro and in vivo evaluations were conducted. In vitro evaluations showed a slight increase in the DNA content of the compression scaffold after 3 days of culture in comparison to the other scaffold, but no difference was noticed after 14 days. In vitro GAG production was also determined resulting in no difference between the scaffolds at all time points. In vivo evaluations in a nude mice subcutaneous model showed that there was an increase in the GAG production in the 3-D fiber deposition scaffolds in comparison to the compression scaffold along with better mechanical integrity. This study suggests that porosity, as well as the scaffold architecture, may play a key role in the OC tissue regeneration.

Following a different approach, Coburn et al. developed a single-phased poly(vinyl alcohol)-methacrylate and low-density chondroitin sulfate methacrylate electrospun nanofiber scaffold that was used to aid chondrogenesis of goat MSCs in vitro [180]. In vitro results showed that the scaffold exhibited an elastic behavior similar to the hyaline cartilage. In addition, further tests showed an increase in cell proliferation and an extensive accumulation of GAG and lacunae formation. To evaluate the in vitro production of both collagen types I and II, immunohistochemical evaluations were conducted and showed an increase in collagen type II production, with no evidence of collagen type I production. This indicates that the addition of chondroitin sulfate methacrylate facilitates the production of collagen type II and had no effects on collagen type I production. In vivo evolutions of the scaffold in a rat OC model revealed that the cell-seeded scaffold had a higher

GAG deposition than the acellular scaffold but had less GAG deposition than normal articular cartilage. Similar to the in vitro study, collagen type II was observed with no evidence to collagen type I in the nanofiber scaffold. Results from this study demonstrate the potential of nanofibers in supporting cartilage regeneration.

Although studies suggest that the single-phased scaffolds can support cellular functions to enhance bone and/or cartilage regeneration, these scaffolds do not mimic the complexity found in the native OC tissue. There has been a serious shift towards the production of bi-phasic and multi-phasic scaffolds to facilitate the regeneration of the different components found in the native OC tissue including the interface. Getgood et al. developed two bi-phasic scaffolds to evaluate their performance at healing the medial femoral condyle and the lateral trochlear sulcus OCDs in a caprine model [183]. The first scaffold was composed of collagen-GAG-calcium phosphate (collagen-GAG-CaP), while the second scaffold was composed of PLGA-PGA. Both scaffolds were implanted on defects made either in the medial femoral condyle or the lateral trochlear sulcus. In vivo evolutions revealed that the collagen-GAG-CaP scaffold became stiffer and provided radical mechanical reinforcement after 12 weeks in comparison to the other scaffold. After 26 weeks, defects treated with collagen-GAG-CaP had a significantly higher content of hyaline cartilage in comparison to defects treated with PLGA/PGA scaffolds, 75–50% respectively. In addition, the Stellar's histological score in the lateral trochlear sulcus was significantly higher when treated with the collagen-GAG-CaP scaffold than PLGA/PGA scaffolds [183].

Chen et al. developed a bi-phasic stratified scaffold [184]. The upper layer of the scaffold for cartilage regeneration was made from collagen sponge, while the lower layer for bone regeneration was made from PLGA 75:25 and naturally derived collagen. To fabricate the porous PLGA-collagen base layer, a particulate-leaching technique was used. Briefly, the scaffold was immersed in collagen type I solution followed by the addition of collagen acidic solution to one side of the scaffold until solidified. The PLGA-collagen scaffold was pre-seeded with bone marrow stromal cells (BMSCs) and cultured for 1 week in vitro prior to an in vivo implantation in a femoral condyle beagle model. Four months after implantation, it was found that cartilage and bone-like tissues were formed in the respective layers. Additional in vivo data revealed that the implant well integrated with the surrounding host tissues suggesting that PLGA-collagen bi-phasic scaffold is useful for OC regeneration.

Growth factors have been also used in combination with scaffolds as a strategic approach for OC regeneration to enhance chondrocyte proliferation and to cue cells to form the specific tissues found in the native OC. Huang et al. developed a PLA/amorphous calcium phosphate (PLA/ACP) hybrid scaffold incorporated with bFGF for OC regeneration [181]. The scaffold was implanted in a femoral condyle OCD in a rabbit model for 4 and 12 weeks. Untreated defects and PLA scaffolds incorporated with bFGF were used as controls. In vivo assessments revealed that the PLA-bFGF-treated defects presented better defect regeneration when compared with the untreated group in all time points. Although PLA-bFGF group showed a good defect regeneration, only low amount of collagen type II and bone formation was observed with a completely negative expression of aggrecan. On the other hand, PLA/ACP-bFGF-treated defects were completely filled with well-established cartilage tissue and cartilaginous ECM after 12 weeks. In addition, an extensive collagen type II production was observed and high levels of aggrecan gene expression were detected.

Growth factors have been also incorporated in a gradient fashion to establish a scaffold for OC interface regeneration. Mohan et al. developed a growth factor gradient scaffold that consisted of TGF-β1 and BMP-2 in combination with PLGA microspheres for OC repair [185]. TGF-β1 was used to establish chondrogenesis at the upper portion of the scaffold, while BMP-2 was used to establish osteogenesis at the lower portion of the scaffold. Combining both factors in a gradient fashion in a single scaffold was based on the hypothesis that the combination of both factors can facilitate the formation of the zonal cartilage and subchondral bone as well as the interface in between. The scaffold was composed of a chondrogenic layer of TGF-β1-loaded PLGA microspheres, and an osteogenic layer of BMP-2 or BMP-2/HA-loaded PLGA microspheres with a gradient transition between both factors in the middle. Blank PLGA scaffold or blank gradient PLGA and PLGA/HA scaffolds were used as controls. Scaffolds were implanted in a medial condyle OCD in a rabbit model for 6 and 12 weeks. It was observed that after 6 and 12 weeks, a great extent of cartilage and subchondral bone similar to those found in the native tissue were achieved in the growth factor–loaded groups when compared with the controls based on the gross morphology, magnetic resonance imaging (MRI), and histological data. In addition, TGF-β1/BMP-2/HA-loaded PLGA microsphere group showed well edge integration with the host bone when compared with all the other groups. These data suggest that incorporating both BMP-2 and HA can facilitate better bone ingrowth and integration to the host bone, whereas TGF-β1 can enhance cartilage regeneration and that the combination of both factors may facilitate the interface regeneration.

Integrating cell-based approaches along with growth factors has also been considered to regenerate OCD. Various cell types have been used to aid in the regeneration of OCD such as progenitor cells and tissue-specific cells such as chondrocytes for cartilage regeneration and osteoblasts for bone regeneration [165]. The small number of chondrocytes found in the cartilage, as well as the difficulties associated with maintaining their phenotype in culture, may present

clinical transitional challenges [189]. In addition, the thorough digestion required to the cartilage matrix by collagenase in order to isolate chondrocytes may be harmful to the cells. Moreover, chondrocytes lose their proliferation capabilities as well as their ability to produce collagen types II and I as soon as the fourth passage is reached by 29,000 folds when compared with the freshly isolated chondrocytes [190]. Due to the aforementioned limitations associated with chondrocytes isolation, maintenance, and usage, many researches shifted to the use of progenitor cells such as stem cells due to their source availability in various body parts, rapid proliferation, and their potential to undergo chondrogenic and osteogenic differentiation, which mark them as ultimately useful for OC regenerative engineering [191].

Cell aggregation at the OCD has been shown to be useful for extracellular matrix synthesis and protein production to support OC tissue regeneration [156]. A novel cell-based approach was studied by Sridharan et al. wherein BMSC aggregates were used for OC regeneration [156]. In this study, different densities of isolated rat BMSC aggregates were encapsulated in fibrin hydrogel and injected in a rat OCD model. Four experimental groups were involved for the in vivo study as follows: fibrin gel encapsulated with high density of BMSC aggregates, low of BMSC aggregates, sham and fibrin hydrogel alone filling the defect. Eight weeks post-implantation, various post vivo evaluations have been conducted in order to evaluate the tissue regeneration including gross morphology observations, hematoxylin and eosin (H&E), Safranin O for GAG production, collagens I and II, and aggrecan immunostaining. Gross morphology analysis showed that fibrin gel encapsulated with high density of BMSC aggregates demonstrated a complete repair to the defect, with much smoother texture surrounding the defect area and color similar to the native cartilage in comparison to the other groups. Immunohistochemistry showed an extensive GAG and collagen type II production with moderate staining of Safranin O in the high-density aggregate group comparing to the low density and fibrin alone. In addition, collagen type I was evident in all groups and stained deeper in the defect filled with high-density aggregates. These recent findings demonstrate the potential of employing cell-based approaches, more specifically, high cellular aggregate densities in facilitating OC tissue regeneration. In this study, fibrin gel encapsulated with high densities of cell aggregates facilitated deep bone formation and full thickness cartilage formation, which suggest that it can be used as a candidate for OC regeneration.

In summary, both stratified and gradient scaffolds in conjunction with growth alone or in combination with cells have been suggested to have significant potential for OC regeneration. Further studies are required in order to prove the capabilities of stratified and gradient scaffold for OC regeneration to accelerate clinical translation.

Conclusion

Different engineering approaches and scaffold designs towards complex tissue regeneration have been employed seeking to recapitulate the graded structural, mechanical, and compositional properties inherited between bone and soft tissues. Based on the various studies discussed here, it is obvious that the traditional tissue engineering approaches of utilizing single-phased scaffold systems are insufficient for recapitulating soft tissue functionality and can poorly achieve graft integration with host tissues. In addition, single-phased scaffold systems do not mimic the complexity found at the native tissue-tissue junctions, leading to negative outcomes towards the formation of tissue-specific interfaces after implantation in vivo. On the other hand, multi-phased scaffold system is more sufficient when it comes to achieving graft integration and physiological functions if topographical and physiologically relevant interface regions are incorporated into the scaffold design, which can be achieved both in stratified and gradient fashions. Regional scaffold cues can also be introduced in order to direct cell fate in the absence of differentiation media both in vitro and in vivo. Spatial patterning in terms of surface chemistry, mechanical properties, or architecture of the underlying substrate has been shown to trigger the differentiation of stem cells to specific targeted tendencies on stratified and gradient scaffolds. Therefore, it is likely that spatial control of relevant inductive factors on the stratified or gradient scaffold is essential to control the fate of the multiple cell populations and direct region-specific matrix development.

Despite the fact that much efforts have been made in this fast-growing field towards the regeneration of complex tissues and their assembly into multi-tissue units, there remain several challenges that need to be carefully addressed. One of the challenges resides on how to ensure the phenotypic maintenance of multiple cellular populations in the heterogeneous cellular environment in vitro, such as determining the optimal culturing media and loading regiment, which are two important factors that can largely affect the phenotypic maintenance and the elaboration of related matrix synthesis. Another challenge is the need of in vitro and in vivo physiologically relevant models to evaluate the clinical transitional potential of these stratified and gradient scaffolds.

This review discusses the various biomimetic engineering approaches and scaffold designs to promote interface tissue regeneration. It is anticipated that these efforts will enable bridging between the distinct tissue types, which can be instrumental towards the regeneration of complex organ systems or a total limb in the near future.

Funding Information This work was funded by the Raymond and Beverly Sackler Center for Biomedical, Biological, Physical and Engineering Sciences, NIH R01AR063698, and NIH DP1 AR068147.

Abbreviations

MSCs, mesenchymal stem cells; hMSCs, human mesenchymal stem cells; BMSCs, bone marrow stromal cells; BMDSCs, bone marrow-derived stem cells; hBMSCs, human bone marrow stem cells; LSPCs, ligament-derived stem/progenitor cells; hTCs, homozygous typing cells; ADSCs, adipose derived stem cells; hADMSCs, human adipose-derived mesenchymal stem cells; ACI, autologous chondrocyte implantation; MACI, matrix-assisted chondrocyte implantation; TGF-β, transforming growth factor beta; TGF-β1, transforming growth factor beta 1; TGF-β3, transforming growth factor beta 3; IGF-I, insulin-like growth factor I; bFGF, basic fibroblast growth factor; BMP-2, bone morphogenetic protein-2; BMP-4, bone morphogenetic protein-4; BMP-7, bone morphogenetic protein-7; PDGF-BB, platelet derived growth factor-BB; PDGF, platelet-derived growth factor; EGF, endothelial growth factor; VEGF, vascular endothelial growth factor; HGF, hepatocyte growth factor; EGF, epidermal growth factor; TH, helioxanthin; SDF-1, stromal cell-derived factor 1; CXCR4, chemokine receptor type 4; GAG, proteoglycans; RUNX2, osteogenic transcription factor-2; PLGA, poly (lactic-co-glycolic acid); PLA, poly(lactic acid); PGA, poly(glycolic acid); PCL, polycaprolactone; PEGT, poly(ethylene glycol); PBT, poly(butylene terephthalate); PNAGA, poly(*N*-acryloyl glycinamide); PU, polyurethane; PC, polycarbonate; PMGI, poly(methylglutarimide); CPC, calcium phosphate cement; TCP, tri-calcium phosphate; β-TCP, beta-tri-calcium phosphate; CaP, calcium phosphate; BG, bioactive glass; ALP, alkaline phosphate; CSF, collagen-silk; HA, hydroxyapatite; ACP, amorphous calcium phosphate; ACL, anterior cruciate ligament; MCL, medial collateral ligament; HS, hamstring tendon; BPTP, bone-patellar tendon-bone; ECM, extracellular matrix; BTJ, bone-tendon junction; MTJ, myotendinous junction; SOT, self-organized tendon constructs; ART, segments of adult; FRT, fetal rat tail; OC, osteochondral; OCD, osteochondral defects; BFM, bipolar electrospun membrane; SFM, simple fibrous membrane; MRCT, massive rotator cuff tears; μCT, micro-computed tomography; MRI, magnetic resonance imaging; SBF, simulated body fluid; 3-D, three-dimensional; microN, maximum isometric force; 3-DFD, 3-D fiber deposition; SLS, selective laser sintering; H&E, hematoxylin and eosin; EDX, energy-dispersive X-ray; CG, collagen-glycosaminoglycan; BMI, body mass index

References

1. Read Frontiers of engineering: reports on leading-edge engineering from the 2012 symposium at NAP.edu. .
2. Qu D, Mosher CZ, Boushell MK, Lu HH. Engineering complex orthopaedic tissues via strategic biomimicry. Ann Biomed Eng. 2015;43(3):697–717.
3. Laurencin CT, Nair LS. The quest toward limb regeneration: a regenerative engineering approach. Regen Biomater. 2016;3(2):123–5.
4. Khademhosseini A, Vacanti JP, Langer R. Progress in tissue engineering. Sci Am. 2009;300(5):64–71.
5. Rao RT, Browe DP, Lowe CJ, Freeman JW. An overview of recent patents on musculoskeletal interface tissue engineering. Connect Tissue Res. 2016;57(1):53–67.
6. Chen T, Jiang J, Chen S. Status and headway of the clinical application of artificial ligaments. Asia-Pac J Sports Med Arthrosc Rehabil Technol. 2015;2(1):15–26.
7. Kobayashi M, Nakagawa Y, Suzuki T, Okudaira S, Nakamura T. A retrospective review of bone tunnel enlargement after anterior cruciate ligament reconstruction with hamstring tendons fixed with a metal round cannulated interference screw in the femur. Arthrosc J Arthrosc Relat Surg. 2006;22(10):1093–9.
8. Gao K, et al. Anterior cruciate ligament reconstruction with LARS artificial ligament: a multicenter study with 3- to 5-year follow-up. Arthrosc J Arthrosc Relat Surg. 2010;26(4):515–23.
9. Matsumoto H, Fujikawa K. Leeds-Keio artificial ligament: a new concept for the anterior cruciate ligament reconstruction of the knee. Keio J Med. 2001;50(3):161–6.
10. Tissue Engineering and Regenerative Medicine | National Institute of Biomedical Imaging and Bioengineering. [Online]. Available: https://www.nibib.nih.gov/science-education/science-topics/tissue-engineering-and-regenerative-medicine. [Accessed: 12-Aug-2019].
11. Machotka Z, Scarborough I, Duncan W, Kumar S, Perraton L. Anterior cruciate ligament repair with LARS (ligament advanced reinforcement system): a systematic review. Sports Med Arthrosc Rehabil Ther Technol SMARTT. 2010;2:29.
12. Samadikuchaksaraei A. Scientific and industrial status of tissue engineering. Afr J Biotechnol. 2007;6:25.
13. Jia Z, Xue C, Wang W, Liu T, Huang X, Xu W. Clinical outcomes of anterior cruciate ligament reconstruction using LARS artificial graft with an at least 7-year follow-up. Medicine (Baltimore). 2017;96(14):e6568.
14. Jia Z-Y, et al. Comparison of artificial graft versus autograft in anterior cruciate ligament reconstruction: a meta-analysis. BMC Musculoskelet Disord. 2017;18(1):309.
15. Atala A. Engineering organs. Curr Opin Biotechnol. 2009;20(5):575–92.
16. Laurencin C and Nair L, Approaches to limb regeneration and other grand challenges.
17. Jeffrey P et al., Volume 12, Issue 12 | Tissue Engineering | Table of Contents. [Online]. Available: http://online.liebertpub.com/toc/ten/12/12. [Accessed: 11-Feb-2018].
18. Moffat KL, Wang I-NE, Rodeo SA, Lu HH. Orthopaedic Interface tissue engineering for the biological fixation of soft tissue grafts. Clin Sports Med. 2009;28(1):157–76.
19. Armitage OE, Oyen ML. Hard-soft tissue interface engineering. Adv Exp Med Biol. 2015;881:187–204.
20. Bayrak E, Yilgor Huri P. Engineering musculoskeletal tissue interfaces. Front Mater. 2018;5.
21. Benjamin M, Evans EJ, Copp L. The histology of tendon attachments to bone in man. J Anat. 1986;149:89–100.
22. Woo SL, Buckwalter JA. AAOS/NIH/ORS workshop. Injury and repair of the musculoskeletal soft tissues. Savannah, Georgia, June 18-20, 1987. J Orthop Res Off Publ Orthop Res Soc. 1988;6(6):907–31.
23. Fujioka H, T. R, and W. G. J, Comparison of surgically attached and non-attached repair of the rat Achilles tendon-bone interface. Cellular organization and type X collagen expression. 1997; pp. 205–218.
24. Rodeo SA, Arnoczky SP, Torzilli PA, Hidaka C, Warren RF. Tendon-healing in a bone tunnel. A biomechanical and histological study in the dog. J Bone Joint Surg Am. 1993;75(12):1795–803.
25. Wang I, Shan J, Chen F, Lu H. Effects of osteoblast and fibroblast interactions on cell growth and differentiation: Biochem Biophys Res Commun; 2006.
26. Frank C, Shrive N, Bray R. Ligament healing: a review of some current clinical and experimental concepts. Iowa Orthop J. 1992;12:21–8.
27. Bray RC, Shrive NG, Frank CB, Chimich DD. The early effects of joint immobilization on medial collateral ligament healing in an ACL-deficient knee: a gross anatomic and biomechanical investigation in the adult rabbit model. J Orthop Res Off Publ Orthop Res Soc. 1992;10(2):157–66.
28. Hart DP, Dahners LE. Healing of the medial collateral ligament in rats. The effects of repair, motion, and secondary stabilizing ligaments. J Bone Joint Surg Am. 1987;69(8):1194–9.

29. Inoue M, McGurk-Burleson E, Hollis JM, Woo SL. Treatment of the medial collateral ligament injury. I: the importance of anterior cruciate ligament on the varus-valgus knee laxity. Am J Sports Med. 1987;15(1):15–21.
30. Ogata K, Whiteside LA, Andersen DA. The intra-articular effect of various postoperative managements following knee ligament repair: an experimental study in dogs. Clin Orthop. 1980;(150): 271–6.
31. Piper TL, Whiteside LA. Early mobilization after knee ligament repair in dogs: an experimental study. Clin Orthop. 1980;150:277–82.
32. Hauser RA. Ligament injury and healing: a review of current clinical diagnostics and therapeutics. Open Rehabil J. 2013;6(1): 1–20.
33. Woo SL, Debski RE, Zeminski J, Abramowitch SD, Saw SS, Fenwick JA. Injury and repair of ligaments and tendons. Annu Rev Biomed Eng. 2000;2:83–118.
34. Fetto JF, Marshall JL. Medial collateral ligament injuries of the knee: a rationale for treatment. Clin Orthop. 1978;132:206–18.
35. Warren RF, Marshall JL. Injuries of the anterior cruciate and medial collateral ligaments of the knee. A long-term follow-up of 86 cases–part II. Clin Orthop. 1978;136:198–211.
36. Yamaji T, Levine RE, Woo SL, Niyibizi C, Kavalkovich KW, Weaver-Green CM. Medial collateral ligament healing one year after a concurrent medial collateral ligament and anterior cruciate ligament injury: an interdisciplinary study in rabbits. J Orthop Res Off Publ Orthop Res Soc. 1996;14(2):223–7.
37. Ohno K, Pomaybo AS, Schmidt CC, Levine RE, Ohland KJ, Woo SL. Healing of the medial collateral ligament after a combined medial collateral and anterior cruciate ligament injury and reconstruction of the anterior cruciate ligament: comparison of repair and nonrepair of medial collateral ligament tears in rabbits. J Orthop Res Off Publ Orthop Res Soc. 1995;13(3):442–9.
38. Frank C, McDonald D, Bray D, Bray R, Rangayyan R, Chimich D, et al. Collagen fibril diameters in the healing adult rabbit medial collateral ligament. Connect Tissue Res. 1992;27(4):251–63.
39. Lo IKY, et al. The cellular networks of normal ovine medial collateral and anterior cruciate ligaments are not accurately recapitulated in scar tissue. J Anat. 2002;200(Pt 3):283–96.
40. Frank C, McDonald D, Shrive N. Collagen fibril diameters in the rabbit medial collateral ligament scar: a longer term assessment. Connect Tissue Res. 1997;36(3):261–9.
41. Hsu S-L, Liang R, Woo SL. Functional tissue engineering of ligament healing. Sports Med Arthrosc Rehabil Ther Technol SMARTT. 2010;2:12.
42. Niyibizi C, Kavalkovich K, Yamaji T, Woo SL. Type V collagen is increased during rabbit medial collateral ligament healing. Knee Surg Sports Traumatol Arthrosc Off J ESSKA. 2000;8(5):281–5.
43. Scheffler SU, Clineff TD, Papageorgiou CD, Debski RE, Ma CB, Woo SL. Structure and function of the healing medial collateral ligament in a goat model. Ann Biomed Eng. 2001;29(2):173–80.
44. Frank C, Woo SL, Amiel D, Harwood F, Gomez M, Akeson W. Medial collateral ligament healing. A multidisciplinary assessment in rabbits. Am J Sports Med. 1983;11(6):379–89.
45. Abramowitch SD, Papageorgiou CD, Debski RE, Clineff TD, Woo SL-Y. A biomechanical and histological evaluation of the structure and function of the healing medial collateral ligament in a goat model. Knee Surg Sports Traumatol Arthrosc Off J ESSKA. 2003;11(3):155–62.
46. Marshall JL, Olsson SE. Instability of the knee. A long-term experimental study in dogs. J Bone Joint Surg Am. 1971;53(8): 1561–70.
47. O'Donoghue DH, Frank GR, Jeter GL, Johnson W, Zeiders JW, Kenyon R. Repair and reconstruction of the anterior cruciate ligament in dogs. Factors influencing long-term results. J Bone Joint Surg Am. 1971;53(4):710–8.
48. Thomopoulos S, Parks WC, Rifkin DB, Derwin KA. Mechanisms of tendon injury and repair. J Orthop Res Off Publ Orthop Res Soc. 2015;33(6):832–9.
49. Deehan DJ, Cawston TE. The biology of integration of the anterior cruciate ligament. J Bone Joint Surg (Br). 2005;87(7):889–95.
50. Lui PP-Y, Zhang P, Chan K-M, Qin L. Biology and augmentation of tendon-bone insertion repair. J Orthop Surg. 2010;5(1):59.
51. Shaerf DA, Pastides PS, Sarraf KM, Willis-Owen CA. Anterior cruciate ligament reconstruction best practice: a review of graft choice. World J Orthop. 2014;5(1):23–9.
52. Cooper JA, Lu HH, Ko FK, Freeman JW, Laurencin CT. Fiber-based tissue-engineered scaffold for ligament replacement: design considerations and in vitro evaluation. Biomaterials. 2005;26(13): 1523–32.
53. Lu HH, Cooper JA Jr, Manuel S, Freeman JW, Attawia MA, Ko FK, et al. Anterior cruciate ligament regeneration using braided biodegradable scaffolds: in vitro optimization studies. Biomaterials. 2005;26(23):4805–16.
54. Cooper JA, Sahota JS, Gorum WJ, Carter J, Doty SB, Laurencin CT. Biomimetic tissue-engineered anterior cruciate ligament replacement. Proc Natl Acad Sci U S A. 2007;104(9):3049–54.
55. Altman GH, Horan RL, Weitzel P, Richmond JC. The use of long-term bioresorbable scaffolds for anterior cruciate ligament repair. J Am Acad Orthop Surg. 2008;16(4):177–87.
56. Kimura Y, Hokugo A, Takamoto T, Tabata Y, Kurosawa H. Regeneration of anterior cruciate ligament by biodegradable scaffold combined with local controlled release of basic fibroblast growth factor and collagen wrapping. Tissue Eng Part C Methods. 2008;14(1):47–57.
57. Samavedi S, Guelcher SA, Goldstein AS, Whittington AR. Response of bone marrow stromal cells to graded co-electrospun scaffolds and its implications for engineering the ligament-bone interface. Biomaterials. 2012;33(31):7727–35.
58. Samavedi S, Vaidya P, Gaddam P, Whittington AR, Goldstein AS. Electrospun meshes possessing region-wise differences in fiber orientation, diameter, chemistry and mechanical properties for engineering bone-ligament-bone tissues. Biotechnol Bioeng. 2014;111(12):2549–59.
59. Spalazzi JP, Dagher E, Doty SB, Guo XE, Rodeo SA, Lu HH. In vivo evaluation of a multiphased scaffold designed for orthopaedic interface tissue engineering and soft tissue-to-bone integration. J Biomed Mater Res A. 2008;86(1):1–12.
60. Spalazzi JP, Doty SB, Moffat KL, Levine WN, Lu HH. Development of controlled matrix heterogeneity on a triphasic scaffold for orthopedic interface tissue engineering. Tissue Eng. 2006;12(12):3497–508.
61. Spalazzi PJ, Moffat LK, and L. HH, Design of a novel stratified scaffold for ACL-to-bone interface tissue engineering., 8th Int. Symp. Ligaments Tendons, 2008.
62. Oh SH, Park IK, Kim JM, Lee JH. In vitro and in vivo characteristics of PCL scaffolds with pore size gradient fabricated by a centrifugation method. Biomaterials. 2007;28(9):1664–71.
63. Li H, Fan J, Sun L, Liu X, Cheng P, Fan H. Functional regeneration of ligament-bone interface using a triphasic silk-based graft. Biomaterials. 2016;106:180–92.
64. Lee-Barthel A, Lee CA, Vidal MA, Baar K. Localized BMP-4 release improves the enthesis of engineered bone-to-bone ligaments. Transl Sports Med. 1(2):60–72.
65. He J, et al. Microfiber-reinforced nanofibrous scaffolds with structural and material gradients to mimic ligament-to-bone interface. J Mater Chem B. 2017;5(43):8579–90.
66. Criscenti G, et al. Triphasic scaffolds for the regeneration of the bone-ligament interface. Biofabrication. 2016;8(1):015009.
67. Hu Y, Ran J, Zheng Z, Jin Z, Chen X, Yin Z, et al. Exogenous stromal derived factor-1 releasing silk scaffold combined with

intra-articular injection of progenitor cells promotes bone-ligament-bone regeneration. Acta Biomater. 2018;71:168–83.
68. Subramony SD, Qu D, Ma R, et al. In vitro optimization and in vivo evaluation of a multiphased nanofiber-based synthetic ACL scaffold. Transactions of the 60th Orthopaedic Research Society. 2014.
69. Cooper RR, Misol S. Tendon and ligament insertion. A light and electron microscopic study. J Bone Joint Surg Am. 1970;52(1):1–20.
70. Matyas JR, Anton MG, Shrive NG, Frank CB. Stress governs tissue phenotype at the femoral insertion of the rabbit MCL. J Biomech. 1995;28(2):147–57.
71. Spalazzi JP, Gallina J, Fung-Kee-Fung SD, Konofagou EE, Lu HH. Elastographic imaging of strain distribution in the anterior cruciate ligament and at the ligament-bone insertions. J Orthop Res Off Publ Orthop Res Soc. 2006;24(10):2001–10.
72. Benjamin M, Toumi H, Ralphs JR, Bydder G, Best TM, Milz S. Where tendons and ligaments meet bone: attachment sites ('entheses') in relation to exercise and/or mechanical load. J Anat. 2006;208(4):471–90.
73. Hems T, Tillmann B. Tendon entheses of the human masticatory muscles. Anat Embryol (Berl). 2000;202(3):201–8.
74. Samavedi S, Olsen Horton C, Guelcher SA, Goldstein AS, Whittington AR. Fabrication of a model continuously graded co-electrospun mesh for regeneration of the ligament-bone interface. Acta Biomater. 2011;7(12):4131–8.
75. Phillips JE, Burns KL, Le Doux JM, Guldberg RE, Garcia AJ. Engineering graded tissue interfaces. Proc Natl Acad Sci. 2008;105(34):12170–5.
76. Engler AJ, Sen S, Sweeney HL, Discher DE. Matrix elasticity directs stem cell lineage specification. Cell. 2006;126(4):677–89.
77. Anitua E, Andia I, Ardanza B, Nurden P, Nurden AT. Autologous platelets as a source of proteins for healing and tissue regeneration. Thromb Haemost. 2004;91(1):4–15.
78. Alsousou J, Thompson M, Hulley P, Noble A, Willett K. The biology of platelet-rich plasma and its application in trauma and orthopaedic surgery: a review of the literature. J Bone Joint Surg (Br). 2009;91(8):987–96.
79. Boswell SG, Cole BJ, Sundman EA, Karas V, Fortier LA. Platelet-rich plasma: a milieu of bioactive factors. Arthrosc J Arthrosc Relat Surg Off Publ Arthrosc Assoc N Am Int Arthrosc Assoc. 2012;28(3):429–39.
80. Pelletier M, Malhotra A, Brighton T, Walsh W, Lindeman R. Platelet function and constituents of platelet rich plasma. Int J Sports Med. 2012;34.
81. Deie M, et al. The effects of age on rabbit MCL fibroblast matrix synthesis in response to TGF-beta 1 or EGF. Mech Ageing Dev. 1997;97(2):121–30.
82. Hildebrand KA, Woo SL, Smith DW, Allen CR, Deie M, Taylor BJ, et al. The effects of platelet-derived growth factor-BB on healing of the rabbit medial collateral ligament. An in vivo study. Am J Sports Med. 1998;26(4):549–54.
83. Murphy PG, Loitz BJ, Frank CB, Hart DA. Influence of exogenous growth factors on the synthesis and secretion of collagen types I and III by explants of normal and healing rabbit ligaments. Biochem Cell Biol. 1994;72(9–10):403–9.
84. Marui T, Niyibizi C, Georgescu HI, Cao M, Kavalkovich KW, Levine RE, et al. Effect of growth factors on matrix synthesis by ligament fibroblasts. J Orthop Res. 1997;15(1):18–23.
85. Scherping SC, Schmidt CC, Georgescu HI, Kwoh CK, Evans CH, Woo SL-Y. Effect of growth factors on the proliferation of ligament fibroblasts from skeletally mature rabbits. Connect Tissue Res. 1997;36(1):1–8.
86. Batten ML, Hansen JC, Dahners LE. Influence of dosage and timing of application of platelet-derived growth factor on early healing of the rat medial collateral ligament. J Orthop Res Off Publ Orthop Res Soc. 1996;14(5):736–41.
87. Schmidt CC, et al. Effect of growth factors on the proliferation of fibroblasts from the medial collateral and anterior cruciate ligaments. J Orthop Res Off Publ Orthop Res Soc. 1995;13(2):184–90.
88. Desrosiers EA, Yahia L, Rivard C-H. Proliferative and matrix synthesis response of canine anterior cruciate ligament fibroblasts submitted to combined growth factors. J Orthop Res. 1996;14(2):200–8.
89. Letson AK, Dahners LE. The effect of combinations of growth factors on ligament healing. Clin Orthop. 1994;308:207–12.
90. Lee J, Green MH, Amiel D. Synergistic effect of growth factors on cell outgrowth from explants of rabbit anterior cruciate and medial collateral ligaments. J Orthop Res. 1995;13(3):435–41.
91. Ito T, Takemasa M, Makino K, Otsuka M. Preparation of calcium phosphate nanocapsules including simvastatin/deoxycholic acid assembly, and their therapeutic effect in osteoporosis model mice. J Pharm Pharmacol. 2013;65(4):494–502.
92. Stadelmann VA, Gauthier O, Terrier A, Bouler JM, Pioletti DP. Implants delivering bisphosphonate locally increase periprosthetic bone density in an osteoporotic sheep model. A pilot study. Eur Cell Mater. 2008;16:10–6.
93. Petrie Aronin CE, Shin SJ, Naden KB, Rios PD Jr, Sefcik LS, Zawodny SR, et al. The enhancement of bone allograft incorporation by the local delivery of the sphingosine 1-phosphate receptor targeted drug FTY720. Biomaterials. 2010;31(25):6417–24.
94. Gellynck K, Shah R, Parkar M, Young A, Buxton P, Brett P. Small molecule stimulation enhances bone regeneration but not titanium implant osseointegration. Bone. 2013;57(2):405–12.
95. Wong E, Sangadala S, Boden SD, Yoshioka K, Hutton WC, Oliver C, et al. A novel low-molecular-weight compound enhances ectopic bone formation and fracture repair. J Bone Joint Surg Am. 2013;95(5):454–61.
96. Yoshii T, Hafeman AE, Esparza JM, Okawa A, Gutierrez G, Guelcher SA. Local injection of lovastatin in biodegradable polyurethane scaffolds enhances bone regeneration in a critical-sized segmental defect in rat femora. J Tissue Eng Regen Med. 2014;8(8):589–95.
97. Monjo M, Rubert M, Wohlfahrt JC, Rønold HJ, Ellingsen JE, Lyngstadaas SP. In vivo performance of absorbable collagen sponges with rosuvastatin in critical-size cortical bone defects. Acta Biomater. 2010;6(4):1405–12.
98. Maeda Y, Hojo H, Shimohata N, Choi S, Yamamoto K, Takato T, et al. Bone healing by sterilizable calcium phosphate tetrapods eluting osteogenic molecules. Biomaterials. 2013;34(22):5530–7.
99. Yamada M, Tsukimura N, Ikeda T, Sugita Y, Att W, Kojima N, et al. N-acetyl cysteine as an osteogenesis-enhancing molecule for bone regeneration. Biomaterials. 2013;34(26):6147–56.
100. Johnson JS, Meliton V, Kim WK, Lee KB, Wang JC, Nguyen K, et al. Novel oxysterols have pro-osteogenic and anti-adipogenic effects in vitro and induce spinal fusion in vivo. J Cell Biochem. 2011;112(6):1673–84.
101. Downing TL, et al. Drug-eluting microfibrous patches for the local delivery of rolipram in spinal cord repair. J Control Release Off J Control Release Soc. 2012;161(3):910–7.
102. Kuo CK, Marturano JE, Tuan RS. Novel strategies in tendon and ligament tissue engineering: advanced biomaterials and regeneration motifs. Sports Med Arthrosc Rehabil Ther Technol SMARTT. 2010;2:20.
103. Yang G, Rothrauff BB, Tuan RS. Tendon and ligament regeneration and repair: clinical relevance and developmental paradigm. Birth Defects Res Part C Embryo Today Rev. 2013;99(3):203–22.
104. Moffat KL, Kwei AS-P, Spalazzi JP, Doty SB, Levine WN, Lu HH. Novel nanofiber-based scaffold for rotator cuff repair and augmentation. Tissue Eng Part A. 2009;15(1):115–26.
105. Moffat KL, Cassilly RT, Subramony SD, et al. In vivo evaluation of a bi-phasic nanofiber-based scaffold for integrative rotator cuff repair. Transactions of the 56th Orthopaedic Research Society. 2010.

106. Zhang X, et al. In vivo evaluation of a biomimetic scaffold in sheep. Trans 60th Annu Meet Orthop Res Soc. 2014.
107. Li X, Xie J, Lipner J, Yuan X, Thomopoulos S, Xia Y. Nanofiber scaffolds with gradations in mineral content for mimicking the tendon-to-bone insertion site. Nano Lett. 2009;9(7):2763–8.
108. Shi J, Wang L, Zhang F, Li H, Lei L, Liu L, et al. Incorporating protein gradient into electrospun nanofibers as scaffolds for tissue engineering. ACS Appl Mater Interfaces. 2010;2(4):1025–30.
109. Dvir T, Timko BP, Kohane DS, Langer R. Nanotechnological strategies for engineering complex tissues. Nat Nanotechnol. 2011;6(1):13–22.
110. Kim J-H, Oh SH, Min HK, Lee JH. Dual growth factor-immobilized asymmetrically porous membrane for bone-to-tendon interface regeneration on rat patellar tendon avulsion model. J Biomed Mater Res A. 2018;106(1):115–25.
111. Li X, Cheng R, Sun Z, Su W, Pan G, Zhao S, et al. Flexible bipolar nanofibrous membranes for improving gradient microstructure in tendon-to-bone healing. Acta Biomater. 2017;61:204–16.
112. Sevivas N, et al. Mesenchymal stem cell secretome improves tendon cell viability in vitro and tendon-bone healing in vivo when a tissue engineering strategy is used in a rat model of chronic massive rotator cuff tear. Am J Sports Med. 2018;46(2):449–59.
113. Font Tellado S, Bonani W, Balmayor ER, Foehr P, Motta A, Migliaresi C, et al. * Fabrication and characterization of biphasic silk fibroin scaffolds for tendon/ligament-to-bone tissue engineering. Tissue Eng Part A. 2017;23(15–16):859–72.
114. Zhu C, Pongkitwitoon S, Qiu J, Thomopoulos S, Xia Y. Design and fabrication of a hierarchically structured scaffold for tendon-to-bone repair. Adv Mater Deerfield Beach Fla. 2018;30(16):e1707306.
115. Park SH, et al. Three-dimensional bio-printed scaffold sleeves with mesenchymal stem cells for enhancement of tendon-to-bone healing in anterior cruciate ligament reconstruction using soft-tissue tendon graft. Arthrosc J Arthrosc Relat Surg Off Publ Arthrosc Assoc N Am Int Arthrosc Assoc. 2018;34(1):166–79.
116. Pham QP, Sharma U, Mikos AG. Electrospinning of polymeric nanofibers for tissue engineering applications: a review. Tissue Eng. 2006;12(5):1197–211.
117. Ma Z, Kotaki M, Inai R, Ramakrishna S. Potential of nanofiber matrix as tissue-engineering scaffolds. Tissue Eng. 2005;11(1–2):101–9.
118. Taylor ED, Nair LS, Nukavarapu SP, McLaughlin S, Laurencin CT. Novel nanostructured scaffolds as therapeutic replacement options for rotator cuff disease. J Bone Joint Surg Am. 2010;92(Suppl 2):170–9.
119. Liu W, et al. Enhancing the stiffness of electrospun nanofiber scaffolds with a controlled surface coating and mineralization. Langmuir ACS J Surf Colloids. 2011;27(15):9088–93.
120. Liu W, Lipner J, Xie J, Manning CN, Thomopoulos S, Xia Y. Nanofiber scaffolds with gradients in mineral content for spatial control of osteogenesis. ACS Appl Mater Interfaces. 2014;6(4):2842–9.
121. Caliari SR, Harley BAC. The effect of anisotropic collagen-GAG scaffolds and growth factor supplementation on tendon cell recruitment, alignment, and metabolic activity. Biomaterials. 2011;32(23):5330–40.
122. Caliari SR, Weisgerber DW, Grier WK, Mahmassani Z, Boppart MD, Harley BAC. Collagen scaffolds incorporating coincident gradations of instructive structural and biochemical cues for osteotendinous junction engineering. Adv Healthc Mater. 2015;4(6):831–7.
123. Platt MA. Tendon repair and healing. Clin Podiatr Med Surg. 2005;22(4):553–60, vi.
124. Benjamin M, Ralphs JR. Tendons and ligaments–an overview. Histol Histopathol. 1997;12(4):1135–44.
125. Shear CR, Bloch RJ. Vinculin in subsarcolemmal densities in chicken skeletal muscle: localization and relationship to intracellular and extracellular structures. J Cell Biol. 1985;101(1):240–56.
126. Bozyczko D, Decker C, Muschler J, Horwitz AF. Integrin on developing and adult skeletal muscle. Exp Cell Res. 1989;183(1):72–91.
127. Swasdison S, Mayne R. Location of the integrin complex and extracellular matrix molecules at the chicken myotendinous junction. Cell Tissue Res. 1989;257(3):537–43.
128. Turner A. Embodied ethnography. Doing culture. Soc Anthropol. 2000;8(1):51–60.
129. Conti HR, Shen F, Nayyar N, Stocum E, Sun JN, Lindemann MJ, et al. Th17 cells and IL-17 receptor signaling are essential for mucosal host defense against oral candidiasis. J Exp Med. 2009;206(2):299–311.
130. Baldino L, Cardea S, Maffulli N, Reverchon E. Regeneration techniques for bone-to-tendon and muscle-to-tendon interfaces reconstruction. Br Med Bull. 2016;117(1):25–37.
131. Structural connections of the muscle-tendon junction, docslide.com.br. [Online]. Available: https://docslide.com.br/documents/structural-connections-of-the-muscle-tendon-junction.html. [Accessed: 11-Feb-2018].
132. Milner T and Kin, Muscle-tendon mechanics, 2001.
133. Kostrominova TY, Calve S, Arruda EM, Larkin LM. Ultrastructure of myotendinous junctions in tendon-skeletal muscle constructs engineered in vitro. Histol Histopathol. 2009;24(5):541–50.
134. Larkin LM, Calve S, Kostrominova TY, Arruda EM. Structure and functional evaluation of tendon-skeletal muscle constructs engineered in vitro. Tissue Eng. 2006;12(11):3149–58.
135. Yang PJ, Temenoff JS. Engineering orthopedic tissue interfaces. Tissue Eng Part B Rev. 2009;15(2):127–41.
136. Bullough, R., et al., Disability and Rehabilitation, in press.
137. Sharma P, Maffulli N. Biology of tendon injury: healing, modeling and remodeling. J Musculoskelet Neuronal Interact. 2006;6(2):181–90.
138. Giovannini S, Brehm W, Mainil-Varlet P, Nesic D. Multilineage differentiation potential of equine blood-derived fibroblast-like cells. Differ Res Biol Divers. 2008;76(2):118–29.
139. Wang JH-C. Mechanobiology of tendon. J Biomech. 2006;39(9):1563–82.
140. Steadman JR, Forster RS, Silferskiöld JP. Rehabilitation of the knee. Clin Sports Med. 1989;8(3):605–27.
141. Zeichen J, van Griensven M, Bosch U. The proliferative response of isolated human tendon fibroblasts to cyclic biaxial mechanical strain. Am J Sports Med. 2000;28(6):888–92.
142. VanDusen KW and Larkin LM, 17 - Muscle–tendon interface, in Regenerative Engineering of Musculoskeletal Tissues and Interfaces, Woodhead Publishing, 2015, pp. 409–429.
143. C. Zhao et al., Preparation of decellularized biphasic hierarchical myotendinous junction extracellular matrix for muscle regeneration, Acta Biomater, vol. 68, pp. 15–28, 01 2018.
144. Ladd MR, Lee SJ, Stitzel JD, Atala A, Yoo JJ. Co-electrospun dual scaffolding system with potential for muscle-tendon junction tissue engineering. Biomaterials. 2011;32(6):1549–59.
145. Merceron TK, et al. A 3D bioprinted complex structure for engineering the muscle-tendon unit. Biofabrication. 2015;7(3):035003.
146. Lu HH, Thomopoulos S. Functional attachment of soft tissues to bone: development, healing, and tissue engineering. Annu Rev Biomed Eng. 2013;15:201–26.
147. Husmann I, Soulet L, Gautron J, Martelly I, Barritault D. Growth factors in skeletal muscle regeneration. Cytokine Growth Factor Rev. 1996;7(3):249–58.
148. Molloy T, Wang Y, Murrell G. The roles of growth factors in tendon and ligament healing. Sports Med Auckl NZ. 2003;33(5):381–94.
149. Moutos FT, Freed LE, Guilak F. A biomimetic three-dimensional woven composite scaffold for functional tissue engineering of cartilage. Nat Mater. 2007;6(2):162–7.

150. Yan L-P, Oliveira JM, Oliveira AL, Reis RL. Current concepts and challenges in osteochondral tissue engineering and regenerative medicine. ACS Biomater Sci Eng. 2015;1(4):183–200.
151. Pearle AD, Warren RF, Rodeo SA. Basic science of articular cartilage and osteoarthritis. Clin Sports Med. 2005;24(1):1–12.
152. Flannery CR, et al. Articular cartilage superficial zone protein (SZP) is homologous to megakaryocyte stimulating factor precursor and is a multifunctional proteoglycan with potential growth-promoting, cytoprotective, and lubricating properties in cartilage metabolism. Biochem Biophys Res Commun. 1999;254(3):535–41.
153. Hunziker EB, Michel M, Studer D. Ultrastructure of adult human articular cartilage matrix after cryotechnical processing. Microsc Res Tech. 1997;37(4):271–84.
154. Venn M, Maroudas A. Chemical composition and swelling of normal and osteoarthrotic femoral head cartilage. I. Chemical composition. Ann Rheum Dis. 1977;36(2):121–9.
155. Muir H, Bullough P, Maroudas A. The distribution of collagen in human articular cartilage with some of its physiological implications. J Bone Joint Surg (Br). 1970;52(3):554–63.
156. Sridharan B, Laflin AD, Holtz MA, Pacicca DM, Wischmeier NK, Detamore MS. In vivo evaluation of stem cell aggregates on osteochondral regeneration. J Orthop Res Off Publ Orthop Res Soc. 2017;35(8):1606–16.
157. Langer R. Biomaterials in drug delivery and tissue engineering: one laboratory's experience. Acc Chem Res. 2000;33(2):94–101.
158. Eyre DR, Wu JJ. Collagen structure and cartilage matrix integrity. J Rheumatol Suppl. 1995;43:82–5.
159. Aigner T, Reichenberger E, Bertling W, Kirsch T, Stöss H, von der Mark K. Type X collagen expression in osteoarthritic and rheumatoid articular cartilage. Virchows Arch B Cell Pathol Incl Mol Pathol. 1993;63(4):205–11.
160. Atala A. Tissue engineering and regenerative medicine: concepts for clinical application. Rejuvenation Res. 2004;7(1):15–31.
161. Bonassar LJ, Vacanti CA. Tissue engineering: the first decade and beyond. J Cell Biochem Suppl. 1998;30–31:297–303.
162. Nukavarapu SP, Dorcemus DL. Osteochondral tissue engineering: current strategies and challenges. Biotechnol Adv. 2013;31(5):706–21.
163. Jiang J, Nicoll SB, Lu HH. Co-culture of osteoblasts and chondrocytes modulates cellular differentiation in vitro. Biochem Biophys Res Commun. 2005;338(2):762–70.
164. Wang I-NE, et al. Role of osteoblast–fibroblast interactions in the formation of the ligament-to-bone interface. J Orthop Res. 2007;25(12):1609–20.
165. Jiang J, Tang A, Ateshian GA, Guo XE, Hung CT, Lu HH. Bioactive stratified polymer ceramic-hydrogel scaffold for integrative osteochondral repair. Ann Biomed Eng. 2010;38(6):2183–96.
166. Cheng H-W, Luk KDK, Cheung KMC, Chan BP. In vitro generation of an osteochondral interface from mesenchymal stem cell-collagen microspheres. Biomaterials. 2011;32(6):1526–35.
167. Martin I, Wendt D, Heberer M. The role of bioreactors in tissue engineering. Trends Biotechnol. 2004;22(2):80–6.
168. Guven S, Chen P, Inci F, Tasoglu S, Erkmen B, Demirci U. Multiscale assembly for tissue engineering and regenerative medicine. Trends Biotechnol. 2015;33(5):269–79.
169. Fergal J, O'Brien. Biomaterials & scaffolds for tissue engineering. 2011;14(3):88–95.
170. Encyclopedia of Polymer Science and Technology, 12 Volume Set, 3rd Edition, Wiley.com. [Online]. Available: https://www.wiley.com/en-us/Encyclopedia+of+Polymer+Science+and+Technology%2C+12+Volume+Set%2C+3rd+Edition-p-9780471275077. [Accessed: 11-Feb-2018].
171. Brown BN, Valentin JE, Stewart-Akers AM, McCabe GP, Badylak SF. Macrophage phenotype and remodeling outcomes in response to biologic scaffolds with and without a cellular component. Biomaterials. 2009;30(8):1482–91.
172. Lyons FG, al-Munajjed AA, Kieran SM, Toner ME, Murphy CM, Duffy GP, et al. The healing of bony defects by cell-free collagen-based scaffolds compared to stem cell-seeded tissue engineered constructs. Biomaterials. 2010;31(35):9232–43.
173. Marler J, Upton J, Langer R, Vacanti J. Transplantation of cells in matrices for tissue regeneration. Adv Drug Deliv Rev. 1998;33(1–2):165–82.
174. Gobbi A, Kon E, Berruto M, Filardo G, Delcogliano M, Boldrini L, et al. Patellofemoral full-thickness chondral defects treated with second-generation autologous chondrocyte implantation: results at 5 years' follow-up. Am J Sports Med. 2009;37(6):1083–92.
175. McNickle AG, Provencher MT, Cole BJ. Overview of existing cartilage repair technology. Sports Med Arthrosc Rev. 2008;16(4):196–201.
176. J. Li, S. Connell, and R. Shi, Biomimetic architectures for tissue engineering, 2010.
177. Kim TG, Shin H, Lim DW. Biomimetic scaffolds for tissue engineering. Adv Funct Mater. 2012;22(12):2446–68.
178. Chu CR, Coutts RD, Yoshioka M, Harwood FL, Monosov AZ, Amiel D. Articular cartilage repair using allogeneic perichondrocyte-seeded biodegradable porous polylactic acid (PLA): a tissue-engineering study. J Biomed Mater Res. 1995;29(9):1147–54.
179. Malda J, Woodfield TB, van der Vloodt F, Wilson C, Martens DE, Tramper J, et al. The effect of PEGT/PBT scaffold architecture on the composition of tissue engineered cartilage. Biomaterials. 2005;26(1):63–72.
180. Coburn JM, Gibson M, Monagle S, Patterson Z, Elisseeff JH. Bioinspired nanofibers support chondrogenesis for articular cartilage repair. Proc Natl Acad Sci U S A. 2012;109(25):10012–7.
181. Huang X, Yang D, Yan W, Shi Z, Feng J, Gao Y, et al. Osteochondral repair using the combination of fibroblast growth factor and amorphous calcium phosphate/poly(l-lactic acid) hybrid materials. Biomaterials. 2007;28(20):3091–100.
182. Dai Y, Shen T, Ma L, Wang D, Gao C. Regeneration of osteochondral defects in vivo by a cell-free cylindrical poly(lactide-co-glycolide) scaffold with a radially oriented microstructure. J Tissue Eng Regen Med. 2018;12(3):e1647–61.
183. Getgood AMJ, et al. Evaluation of early-stage osteochondral defect repair using a biphasic scaffold based on a collagen-glycosaminoglycan biopolymer in a caprine model. Knee. 2012;19(4):422–30.
184. Chen G, Sato T, Tanaka J, Tateishi T. Preparation of a biphasic scaffold for osteochondral tissue engineering. Mater Sci Eng C. 2006;26(1):118–23.
185. Mohan N, Dormer NH, Caldwell KL, Key VH, Berkland CJ, Detamore MS. Continuous gradients of material composition and growth factors for effective regeneration of the osteochondral interface. Tissue Eng Part A. 2011;17(21–22):2845–55.
186. Liao J, et al. The fabrication of biomimetic biphasic CAN-PAC hydrogel with a seamless interfacial layer applied in osteochondral defect repair. Bone Res. 2017;5:17018.
187. Gao F, et al. Direct 3D printing of high strength biohybrid gradient hydrogel scaffolds for efficient repair of osteochondral defect. Adv Funct Mater. 28(13):1706644.

188. Du Y, et al. Selective laser sintering scaffold with hierarchical architecture and gradient composition for osteochondral repair in rabbits. Biomaterials. 2017;137:37–48.
189. Csaki C, Schneider PR, Shakibaei M. Mesenchymal stem cells as a potential pool for cartilage tissue engineering. Ann Anat Anat Anz Off Organ Anat Ges. 2008;190(5):395–412.
190. Fröhlich M, Maličev E, Gorenšek M, Knežević M, Kregar Velikonja N. Evaluation of rabbit auricular chondrocyte isolation and growth parameters in cell culture. Cell Biol Int. 2007;31(6):620–5.
191. P. S in 't Anker et al., Mesenchymal stem cells in human second-trimester bone marrow, liver, lung, and spleen exhibit a similar immunophenotype but a heterogeneous multilineage differentiation potential, Haematologica, vol. 88, pp. 845–52, Aug. 2003.